

8870

NACA TN 2480

0065578

TECH LIBRARY KAFB, NM

NATIONAL ADVISORY COMMITTEE FOR AERONAUTICS

TECHNICAL NOTE 2480

COMPARISON OF HEAT TRANSFER FROM AIRFOIL IN NATURAL
AND SIMULATED ICING CONDITIONS

By Thomas F. Gelder and James P. Lewis

Lewis Flight Propulsion Laboratory
Cleveland, Ohio



Washington

September 1951

AFM3C

TECHNICAL LIBRARY

AFL 2811



0065578

NACA TN 2480

NATIONAL ADVISORY COMMITTEE FOR AERONAUTICS

TECHNICAL NOTE 2480

COMPARISON OF HEAT TRANSFER FROM AIRFOIL IN NATURAL
AND SIMULATED ICING CONDITIONS

By Thomas F. Gelder and James P. Lewis

SUMMARY

An investigation of the heat transfer from an airfoil in clear air and in simulated icing conditions was conducted in the NACA Lewis 6- by 9-foot icing-research tunnel in order to determine the validity of heat-transfer data as obtained in the tunnel. This investigation was made on the same model NACA 65,2-016 airfoil section used in a previous flight study, under similar heating, icing, and operating conditions.

The effect of tunnel turbulence, in clear air and in icing, was indicated by the forward movement of transition from laminar to turbulent heat transfer. An analysis of the flight results showed the convective heat transfer in icing to be considerably different from that measured in clear air and only slightly different from that obtained in the icing-research tunnel during simulated icing.

INTRODUCTION

The determination of the heat required for the protection of aircraft in icing has been the subject of considerable research by the NACA for a number of years. For specific aircraft, the heat required to realize an arbitrary temperature rise above the free-stream air temperature of the airplane surfaces that are subject to icing is determined in reference 1. The development by Hardy (reference 2) of an analysis of the heat transfer from an airplane surface during icing provides a means of computing the heat requirements for specified icing conditions. The flight tests reported in reference 3 provide results for limited conditions, which, in general, substantiate the analysis of Hardy.

Icing investigations conducted in flight are difficult to control and time consuming. An investigation of the heat transfer from an airfoil in clear air and in icing over a range of controlled conditions was therefore conducted in the NACA Lewis icing-research tunnel.

A comparison of the heat-transfer results obtained in the icing-research tunnel with those obtained in flight using the same model airfoil and operating at similar conditions is presented herein.

DESCRIPTION OF EQUIPMENT

The model used in the tunnel investigation was an NACA 65,2-016 airfoil section having an 8-foot chord and a 6-foot span. With minor modifications required for the tunnel installation, it was the same model used in a flight investigation in natural icing conditions and is fully described in reference 3. The airfoil was vertically mounted in the tunnel as shown in figure 1. Construction details of the 1-foot span electrically heated test section are given in figure 2. The 20 groups of heating elements in this area were arranged into 11 electric circuits selected to provide the most flexible chordwise adjustment of power distribution within the limits of the available facilities. The differences in power readings for heating elements common to the same circuit are caused by differences in resistance. This arrangement permitted a chordwise power distribution similar to that employed in the flight investigations. The heated length of the test strip extended to 55 percent of the chord length on the left side of the airfoil and to 17 percent of the chord length on the right side.

The span of the model was increased from 4.7 to 6 feet for the tunnel installation. The guard sections above and below the test strip consisted of 0.125-inch aluminum skin and were heated by woven wire heating blankets cemented to the inner surface of the skin. These blankets were designed to provide the same heating power distribution used in the flight investigations. The heated length of the guard sections extended to 17 percent of the chord length on both surfaces of the airfoil.

The temperatures of the external skin and the model interior were obtained by means of iron-constantan thermocouples and were recorded by means of self-balancing automatic potentiometers. The installation and the location of the thermocouples are described in reference 3.

The flow of heat from the electric-resistance heating elements was determined from wattmeter measurements of the power applied minus all calculated lead losses determined from measured lead resistances and currents. A source of 208-volt, 60-cycle, three-phase alternating current was supplied to the model through variable autotransformers.

The pressure distribution over the surface of the model in the tunnel was measured by means of flush pressure taps located in the test strip. The pressures were indicated on a multiple-tube manometer and photographically recorded.

2175 Simulated icing conditions were obtained in the test section of the tunnel by introducing liquid water into the air stream from eight NACA air-atomizing nozzles placed in four steam-heated struts located upstream of the tunnel test section. Initially the spray system was placed in the tunnel contraction section approximately 22 feet upstream of the model. For most of the investigation, the spray nozzles were located in the low-velocity section of the tunnel with a mixing distance from the nozzles to the model of 48 feet (fig. 3). The liquid-water content of the icing cloud was varied from approximately 0.3 to 1.5 grams per cubic meter by adjusting the nozzle water pressure; the mean-effective droplet diameter was varied from about 8 to 12 microns by adjusting the nozzle-air pressure. Liquid-water content, droplet size, and droplet-size distribution were determined by the rotating multicylinder method described in reference 4. The droplet-size distributions given in table I and defined in reference 4 are arbitrary size-frequency distributions based on measurements in natural icing with the A distribution denoting droplets of a single size.

PROCEDURE

In the initial phase of this investigation, the velocity distribution over the airfoil was determined with the airfoil chord line set at an angle of attack of 0° and over a speed range sufficient to include that employed in the flight investigation.

Prior to the simulated flight investigations in the icing-research tunnel, a study was made of the effects of the tunnel and the inoperative spray system on the heat transfer from the model. This study was conducted in clear air with (1) the spray system removed from the tunnel air stream, (2) the spray system approximately 22 feet upstream of the model, and (3) the spray system 48 feet upstream of the model. The remainder of the tunnel investigations were conducted with the spray system at the 48-foot mixing-distance location.

The general procedure followed in the investigation was to stabilize all model and tunnel conditions and to record all appropriate data before applying heat to the model and before introducing water into the air stream. Heat was then applied to the model and a complete record of data was taken upon stabilization of the model temperatures. The water sprays were then turned on and data were recorded.

after all conditions and model temperatures had stabilized. The tunnel airspeed and temperature were maintained constant during each condition. Frequent checks of the spray cloud were made during the icing period by introducing the 1/8-inch cylinder of the rotating multi-cylinder assembly into the cloud and comparing this measurement with that obtained during the calibration of the spray system. Photographs of the model and any ice accretions were taken immediately following the investigation of each condition.

The icing investigation was divided into two phases: (1) The heating-power distributions to the test strips were adjusted to approximate closely those employed in the flight investigations and studies were made at operating and icing conditions similar to those encountered in flight; (2) the heating-power distributions were readjusted to produce uniform surface temperatures both in clear air and in simulated icing.

The degree of surface wetness of the test strip was determined in the tunnel at above freezing air temperatures by wrapping a sheet of acetate film, which had a water-sensitive coating, around the leading edge of the unheated airfoil; a permanent record of the water impingement and runback on the model surface was thus obtained. Film was used because it is less absorbent than paper; therefore, the flow conditions on the metal skin could be more closely approximated.

METHOD OF ANALYSIS AND CALCULATION

The analysis used in this investigation is essentially the same as that presented in reference 3. The equation for heat transfer from a heated-airfoil surface during an icing condition, which is presented in reference 3, may be written

$$q = q_m + q_c + q_e \quad (1)$$

(All symbols are defined in the appendix.) If the expressions for component heat losses are substituted in equation (1), the total heat loss becomes

$$q = M_a \left[t_s - (t_0 + \Delta t_w) \right] + h_c (t_s - t_{a,w}) + h_c (X-1) (t_s - t_{a,w}) \quad (2)$$

The term Δt_w is the kinetic temperature rise of the impinging water and can be expressed by

$$\Delta t_w = \frac{v^2}{2gJc_{p,w}}$$

where $c_{p,w}$ is the specific heat of water at constant pressure, equal to 1.0 Btu per pound per $^{\circ}\text{F}$. This temperature rise amounts to less than 2°F for speeds less than 200 miles per hour and is neglected in this analysis. The surface-datum temperature in clear air $t_{a,d}$ is defined as

$$t_{a,d} = t_0 + \frac{v^2}{2gJc_p} \left[1 - \left(\frac{U}{V} \right)^2 \left(1 - N_{Pr}^n \right) \right] \quad (4)$$

The equation for surface-datum temperature in wet air (reference 2) may be written

$$t_{a,w} = t_0 + \frac{v^2}{2gJc_p} \left[1 - \left(\frac{U}{V} \right)^2 \left(1 - N_{Pr}^n \right) \right] - 0.622 \frac{L}{c_p} \left(\frac{e_{a,w} - e_1}{p_1} \right) \quad (5)$$

The evaporation factor X given by Hardy in reference 5 is written

$$X = 1 + \frac{L}{c_p} \left(\frac{e_s - e_{a,w}}{t_s - t_{a,w}} \right) \frac{0.622}{p_1} \quad (6)$$

This expression is applicable only in that region in which the surface is fully wetted. For the region in which the surface is not fully wetted, the evaporative term must be modified by the factor K to account for this partial wetness; therefore,

$$q_e = h_c K (X-1) (t_s - t_{a,w}) \quad (7)$$

Thus, the equations for the external heat transfer from the airfoil surface for the conditions of clear air and in a cloud, respectively, are

$$q_d = h_c(t_s - t_{a,d}) \quad (8)$$

and

$$q_w = M_a(t_s - t_0) + h_c(t_s - t_{a,w}) [1 + K(X-1)] \quad (9)$$

In this report, equations (8) and (9) were solved for the convective heat-transfer coefficient h_c , which is then used as a basis of correlation and comparison of the tunnel and flight investigations. The unit rate of heat flow q from the surface was determined from the measured heat values applied to each element minus the internal heat loss obtained from the measured temperatures underneath the heating elements. Measured surface temperatures were used for the term t_s .

The weight rate of water-droplet impingement per unit area M_a was computed from the measured values of liquid-water content, droplet size, velocity, temperature, and pressure using the computed trajectories for a symmetrical, 12-percent-thick Joukowski airfoil as given in reference 3. No water-droplet collection efficiencies were available for the NACA 65,2-016 section and hence the values from the Joukowski trajectories were used as the most applicable of those available.

The free-stream static air temperature t_0 was determined for the tunnel data from the measured surface-datum temperatures in clear air $t_{a,d}$ and equation (4) and was checked by measurements of the tunnel total temperature using the relation

$$t_0 = t_T - \frac{v^2}{2gJc_p} \quad (10)$$

The results agreed within the limits of accuracy of temperature measurements.

For comparison, the following analytical expressions for the convective heat-transfer coefficient given in reference 6 were used:

For flat-plate laminar flow

$$N_{Nu} = \frac{h_c s}{k} = 0.332 N_{Pr}^{1/3} N_{Re,s}^{0.5} \quad (11)$$

For flat-plate turbulent flow

$$N_{Nu} = \frac{h_c s}{k} = 0.0296 N_{Pr}^{1/3} N_{Re,s}^{0.8} \quad (12)$$

In addition, the expression for convective heat transfer from a flat plate with a laminar boundary, in which a more exact account is taken of the pressure gradient, is given by

$$N_{Nu} = F_7 N_{Pr}^{1/3} N_{Re,s}^{0.5} \quad (13)$$

where F_7 is a correlation factor that is a function of the Euler number, m ($m = \frac{s}{U} \frac{dV}{ds}$), and Prandtl number. The relations between F_7 , m , and N_{Pr} are obtained by use of equations given in reference 7.

RESULTS

The operating and icing conditions for the flight and the icing-research-tunnel investigations are presented in table I. The first five conditions listed in table I of this report are those of specific flights taken from reference 3, which are used for comparing the heat transfer from an airfoil in natural and in simulated icing. Conditions 6 through 9' are from icing-research-tunnel investigations in which the flight heating distributions were employed. Conditions 10, 11', 12', 13', and 14' are tunnel investigations in which the heating distribution was adjusted to provide a uniform surface temperature.

Velocity Distribution

The velocity distribution for an angle of attack of 0° as measured in flight and in the icing-research tunnel is shown in figure 4. Good correlation of the tunnel values corrected for tunnel effects with the

theoretical velocity distributions was obtained. The uncorrected values, however, were used in the heat-transfer calculations as representing the true local velocity over the airfoil surface during the tunnel investigations.

Surface-Datum Temperature

For the flight tests, the experimental surface-datum temperatures are not reported. In the icing-research tunnel, the surface-datum temperatures were measured in clear air for each operating condition. A comparison of the surface-datum temperatures measured in the icing-research tunnel in clear air with the value calculated from equation (4) is shown in figure 5 for condition 10'. The measured temperatures vary as much as 2° F from the calculated values, which is within the accuracy of measurement.

The datum temperatures in a cloud that is below freezing cannot be measured directly because of the release of heat by the freezing of the impinging water. For the flight conditions, the wet-datum temperatures were computed from equation (5). For tunnel conditions, the wet datum temperatures were calculated by deducting the temperature depression caused by evaporation from an average of the measured clear-air surface-datum temperatures.

Impingement and Evaporation

Records of the impingement and the water flow over the airfoil surface were obtained by placing a water-sensitive material on the forward portion of the airfoil model. Typical records of this type are shown in figure 6. The results obtained in the tunnel and in flight were substantially the same. The solid areas on the records of figure 6 are the regions of direct water impingement in which the surface was fully wetted. Downstream of the limit of direct impingement the water breaks into individual streams or rivulets that tend to decrease in size and number. The weight rate of water impingement for one side of the airfoil model in pounds per hour per foot span and the limits of impingement were calculated for each condition by use of the water-droplet trajectories for a symmetrical, 12-percent-thick Joukowski airfoil. The results of these calculations are given in table II.

2175

In the partly wetted area downstream of direct impingement, the rate of evaporation per unit area is less than in the fully wetted area. In the absence of detailed knowledge of the evaporation process in this partly wetted area, the full evaporation rate was decreased by a factor equal to the percentage of the total surface area that is actually wetted. From the flight and the tunnel records of impingement and runback as shown in figure 6, the actual area wetted by the runback rivulets was measured at various surface distances downstream of the limits of impingement. The results of these measurements are shown in figure 7. The wetness factor K decreases sharply from a value of 1 at the limit of impingement to a mean value of approximately 25 percent 1-inch downstream of the impingement limit and decreases slowly thereafter. The tunnel and flight measurements show agreement, which indicates that the flow process is substantially the same. Within the range of conditions investigated, no significant variation of the wetness factor with limit of impingement was noted. The actual degree of wetness probably does not follow a smooth curve. Although figure 6 reveals that several of the rivulets either stop or merge rather abruptly, in the heat-transfer calculations of this report the wetness factor was regarded as continuously decreasing with distance as indicated in figure 7. Further refinement does not appear warranted from the data and lack of information regarding the evaporation process in this runback area. The calculated rates of evaporation and the limits of runback for each of the flight and the tunnel icing conditions are presented in table II.

Effect of Tunnel and Spray System in Clear Air

The initial heat-transfer measurements in the icing tunnel were made in clear air in order to determine the effect of the tunnel and the inoperative spray system on the convective heat-transfer coefficient. The results of these measurements are given in figure 8, which presents the heat flow from the surface, the heated and unheated surface temperatures, and the convective heat-transfer coefficient. The heat distribution used was experimentally determined as that producing an approximately uniform surface temperature.

When the spray system was not in the tunnel (fig. 8), raising the tunnel true airspeed from 138 to 194 miles per hour had no measurable effect on the location of the minimum convective heat-transfer coefficient, which remained at about 8-percent chord, whereas the location of the maximum coefficient moved forward from approximately 28- to 24-percent chord.

The tunnel results, that were obtained in clear air, are also presented in the conventional nondimensional Nusselt form in figure 9(a). The flight results in clear air (condition 5') are similarly presented for comparison in figure 9(b). In addition to the experimental data, the analytical expressions for the flat plate have been plotted in these figures. In flight in clear air (fig. 9(b)), laminar transfer is obtained over a considerable portion of the airfoil with good correlation occurring between the experimental data and the flat-plate laminar expression, in which the Euler parameter (equation (13)) is used. Transition started at a local Reynolds number $N_{Re,s}$ of approximately 2.3×10^6 . The sharp transition resulted in full turbulent transfer being obtained at a local Reynolds number of approximately 3×10^6 . Good correlation with the turbulent analytical curves was obtained. The first few points in the turbulent region are believed to be above the analytical curve because of unaccounted for conduction effects inside the airfoil heater inasmuch as a sudden increase in the power occurred at this point.

All the tunnel data obtained in clear air with the spray system removed from the air stream (conditions 12' and 13') are presented in a Nusselt plot in figure 9(a). In the region of $2 \times 10^5 < N_{Re,s} < 1.1 \times 10^6$, the experimental data lie considerably above but approximately parallel to the analytical laminar curves. These results, which hereinafter will be referred to as "semilaminar heat transfer," are approximately 40 and 65 percent higher than those indicated by equations (13) and (11), respectively. This effect may possibly be caused by the turbulence level of the tunnel. No honeycombs or screens were employed to reduce the tunnel turbulence, which is believed caused in large measure by the tunnel refrigeration coils located just upstream of the first corner forward of the test section. In figure 9(a), transition starts at a local Reynolds number of approximately 1.1×10^6 . The data of figure 9(b) show some evidence of instability occurring at approximately this local Reynolds number. Transition in the tunnel took place more gradually than in flight, with full turbulence reached at a local Reynolds number of approximately 3.5×10^6 . As in the case of laminar transfer, the tunnel turbulent heat transfer is larger than the analytical value. This difference of approximately 30 percent is again probably caused by turbulence in the tunnel. The two conditions shown in figure 9(a) differ by 56 miles per hour but no change in the local Reynolds number of transition is apparent.

In an effort to obtain a suitable spray cloud in the test section of the icing-research tunnel, the spray system was installed at two positions in the tunnel air stream (22 and 48 ft upstream of the model). These two positions gave different amounts of stream turbulence and

2175 therefore measurements of the heat transfer from the airfoil model were made at each position with the spray system inoperative. The Nusselt plots of the results for these conditions are given in figure 9(c). The data in the laminar region again lie above the theoretical curves. Transition begins at a local Reynolds number of approximately 5×10^5 and 9×10^5 for the 22 and 48 foot positions, respectively. These values of local Reynolds number correspond to chord distances of 4 and 12 percent, respectively. The transition curve is slightly steeper for the 48-foot position with the full turbulent value being attained at a local Reynolds number of 2.5×10^6 as compared with a value of 1.3×10^6 at the 22-foot position of the spray system.

All the faired curves for the icing-research tunnel and the flight clear-air investigations employing a uniform surface temperature are compared in figure 10. The tunnel semilaminar data all fall very close together. The effect of increasing the turbulence level of the tunnel was to cause initiation of transition at a smaller Reynolds number.

Tunnel Simulations of Flight Icing

The investigations in the icing-research tunnel, in which heat distributions similar to those used in flight were employed, were made at approximately the same true airspeed and free-stream air temperatures encountered in flight, but because the icing-research tunnel is an atmospheric tunnel, it was impossible to simulate the flight pressure-altitudes resulting in slightly larger Reynolds numbers for the tunnel data. Because the rate and the distribution of water impingement is primarily dependent on velocity, the tunnel true airspeed was set to simulate flight velocity in order to approach the same impingement.

Typical results of the icing-research tunnel simulations of flight heating distribution and operating conditions for both clear air and icing are given in figure 11, (conditions 8 and 8'). The most important result shown in figure 11 is the large heated-surface temperature gradient resulting from the use in the turbulent tunnel air stream of a heat distribution designed to obtain uniform surface temperatures in clear-air flight. The pronounced effect of the impinging water and evaporation on the heated-surface temperatures is also apparent particularly near the leading edge.

The results of icing tunnel simulations of flight in clear air and in icing are given in Nusselt correlation form in figure 12 (conditions 6 to 9'). Lack of sufficient and accurate data in the extreme leading-edge region precluded the fairing of the curves at values of $N_{Re,s}$ less than approximately 2.5×10^5 . In general, the results in clear air (fig. 12) are quite similar to those shown in figure 9(c). Prior to transition, the clear-air results of figure 12 follow a curve having the same slope as the theoretical laminar curve, but with values of Nusselt number that are considerably larger. These semilaminar curves for the clear-air results of figure 12 are slightly lower than the corresponding results of condition 11' (fig. 9(c)), which were obtained with the spray system in the same position but at a greater true airspeed and with a uniform surface temperature. In figure 12, the faired curves in the region of semilaminar transfer are in agreement with the variation for the four conditions (6', 7', 8', and 9', table I), being approximately ± 7 percent, which is within the scatter of the data. The slopes of the clear-air transition curves of figure 12 are less than those of figure 9(c). This effect appears to be the result of the combination of differences in airspeed and surface temperature. Following transition, fully turbulent heat transfer is obtained at a local Reynolds number of approximately 4×10^6 in each condition. The sharp peak at a local Reynolds number of approximately 5×10^6 and the subsequent increased turbulent values are attributed in part to the sudden increase in temperature and heat input at this point.

The results shown in figure 12 for simulated icing (conditions 6, 7, 8, and 9) were obtained by keeping all tunnel conditions the same as for clear air and exposing the airfoil model to the icing cloud. The icing and the clear-air curves are somewhat similar in shape although much greater differences in the value of the Nusselts-number parameter between the various conditions are apparent and transition in every case occurs at a lower local Reynolds number in the icing condition. Because of the limited data, it is impossible to correlate fully the results with the icing variables of rate of impingement, limit of impingement, amount evaporated in the impingement area, and amount of water running back. In icing as in clear air, no true laminar heat transfer is obtained. With the exception of condition 8, transition started at a local Reynolds number of less than 3×10^5 . In calculating the results for conditions 7 and 9, it was found that partial wetness occurred before the calculated limit of impingement. This result is attributed to errors in the wetness factor assumed and to the fact that the actual effective limit of impingement is smaller than that calculated by the available trajectories for a symmetrical, 12-percent-thick Joukowski airfoil. The presence of ice and its location on the surface also have an appreciable effect on the transition curve as shown by a comparison of the icing results of figures 12(a) and 12(c), which are conditions having approximately the same calculated rate of

2175
water impingement and limit of impingement. Ice on the surface and the nature of the heat distribution also complicate the determination of the point of full turbulent heat transfer. As in the case of clear-air results with the flight heat distribution, the data show a sharp peak at a local Reynolds number of approximately 5×10^6 , which corresponds to the position at which a sharp increase occurs in power input to the heater.

Photographs of ice that formed on the airfoil surface are shown in figure 13. These ice formations were the result of the combination of the free-stream air temperature, the cooling because of evaporation, and the forward movement of transition causing the surface temperature to fall below 32°F .

Flight Results

The results of the flight investigation reported in reference 3 are presented in the Nusselt correlation form in figure 14. Curves of estimated Nusselt parameter corresponding to a fully wetted surface ($K = 1.0$) and a completely dry surface ($K = 0$) are shown for comparison. For a completely wetted surface, the value of X based on the measured surface temperatures was used in the solution of equation (9). If the surface is assumed to be completely dry, the evaporative term disappears from the equation. All the experimental results using the partial wetness factor of figure 7 should lie between these two limiting curves. The data points should also lie on the lower curve in the region of direct impingement where the surface is fully wetted and then gradually approach the upper curve as the water is evaporated. The scatter of the data and the shape of the faired Nusselt curve thus give an indication of the accuracy of the original assumptions as to the wetness factor K based on the runback measurements of figure 7. These flight results show certain differences from those obtained in the icing-research tunnel under a similar chordwise heat distribution. The greatest variation is in the region of a local Reynolds number of 6×10^5 . For two of the four conditions reported, full laminar transfer is attained up to a local Reynolds number of 4×10^5 with good correlation with equation (13) resulting. No laminar transfer was obtained for condition 3, (fig. 14(c)); this condition had the limit of impingement nearest the leading edge.

Comparison of the flight results indicates an almost direct relation between the limit of impingement and the extent of laminar flow. Beyond the laminar region, the experimental curves rise abruptly and for the rest of the transition region resemble the tunnel results

fairly closely. The shape of the curves in the transition region is probably caused by surface temperatures, heat gradients, and inaccurate assumptions as to the rate and extent of water impingement and the partial wetness factor. Obtaining a smooth transition curve with no reversal requires that the wetness factor change by a factor of 3 to 4 times that used and would result in the surface becoming dry at local Reynolds numbers of 10^6 or less. This effect is not supported by observations and would require the calculated rate of water impingement to be in error by a factor of 1.4 to 1.7. Such variations appear, however, to be unreasonable and it is believed that the data of figure 14 represent the transition occurring in flight. The steep rise at the beginning of transition for the flight results is attributed to the breaking up of the water film into rivulets and the resultant partial evaporation. This effect is more pronounced in flight data than in tunnel data because of the superimposition of the tunnel-stream turbulence. The reversal in the curve is probably caused in part by the negative surface-temperature gradients, which would tend to delay the transition to full turbulent transfer. An exact evaluation of these effects cannot be made in place of measurements of the temperature profiles and rates of evaporation by means of boundary-layer studies. The sharp peak near the completion of transition obtained in the icing-research-tunnel studies was also obtained in flight although it did not rise as high above the analytical turbulent curve.

Additional Tunnel Results

In addition to the tunnel investigation in which the flight heat distribution was used, studies were made with heat distributions that gave uniform surface temperatures in clear air and also in simulated icing. The results obtained with a uniform surface temperature in clear air in the icing-research tunnel have already been presented in figure 9(c). The thermal data obtained with this same heat distribution during icing in the tunnel are given for condition 11' in figure 15. The original surface temperature, which was approximately 70° F in clear air, was sharply reduced in the first 20 percent of chord and a minimum temperature of -25° F was obtained, which resulted in ice formations. Photographs of these ice formations are shown in figure 16. The heat-transfer results are presented in the Nusselt correlation form in figure 17(a) together with a comparison with the clear-air curve. A marked forward movement of transition resulted from operation in icing with the actual transition beginning at approximately 2 percent of chord (fig. 15). The turbulent curve downstream of the ice formation follows the slope of the theoretical turbulent curve from equation (12), but is approximately 18 percent higher than the curve obtained in clear air at the same condition.

2175 The airfoil model was also operated with the heat distribution modified to produce a uniform surface temperature during an icing condition. The operating conditions were held approximately constant with the exception of the liquid-water content, which was increased to insure that the entire heated surface would be wet. The surface temperature was lowered to a uniform value slightly above freezing (35°F) to minimize the effects of evaporation. These results (condition 10) together with those obtained with the same heat distribution in clear air (condition 10') are given in figure 17(b). These icing results correlate closely with those of condition 11 (fig. 17(a)). The clear-air results of figure 17(b) are similar to those obtained using the flight heat distribution in clear air in the icing tunnel and are characterized by a region of semilaminar transfer up to a local Reynolds number of approximately 7×10^5 followed by a very gradual transition.

A comparison of the tunnel results for conditions 10, 10', 11, and 11' for both clear air and icing is presented in figure 18. The effects of the surface-temperature distribution in changing the point of initiation and rate of transition are shown to be relatively minor as compared with the difference between clear air and icing. All the experimental turbulent values agree with each other within approximately 15 percent, but average about 30 percent larger than the theoretical values from equation (12).

Comparison of Tunnel and Flight Results

A comparison of the tunnel and flight results is shown in figure 19 for icing conditions 1 and 8. These conditions had approximately the same true airspeed, free-stream temperature, and limit of impingement; the same flight heat distribution that resulted in non-uniform surface temperatures in icing was used for both. No comparison is made for the case of uniform surface temperatures in icing inasmuch as such results were not obtained in the flight investigation. The greatest discrepancy between the tunnel and flight results of figure 19 occurs in the laminar region at a local Reynolds number of 3×10^5 and in the turbulent region at a local Reynolds number of 3×10^6 where large peaks for both flight and tunnel result from sudden increases in heat input at this region. In the transition region, a better comparison is obtained; the tunnel results are approximately 5 to 30 percent higher than the flight results. The data for these two conditions (figs. 14(a) and 12(c)) show a scatter of approximately 15 percent during transition. In the turbulent region, the results agree within 10 percent except for the large peaks caused by the discontinuity of the heat distribution.

The requirements of a thermal ice-protection system based upon the tunnel results will be conservative as shown by a consideration of equation (9). The convective heat-transfer coefficients obtained in the icing tunnel are consistently higher than those obtained in flight. The amount by which the heat requirements are conservative cannot be evaluated directly, being dependent on the specific conditions of interest, principally the surface temperature, rate of heating, free-stream air temperature and velocity, and the type of heating system. Because of the limitations of this investigation, the heat-transfer relation that exists over a wide range of airspeeds, free-stream and surface temperatures, rates and types of heating, angles of attack, and body configurations were not determined. In general, it would appear that for bodies in which the heated area is confined to a small area near the leading edge or in which transition is delayed considerably, the tunnel results may give excessive heat requirements. For bodies in which the heated area is a larger percentage of the total area or in which transition is initiated early, the tunnel requirements will be only slightly conservative.

SUMMARY OF RESULTS

The results of the investigation of heat transfer from an airfoil in the icing-research tunnel may be summarized as follows:

1. The pattern of the runback rivulets and hence the degree of surface wetness were substantially the same for both the tunnel and flight results.
2. The inherent turbulence level of the tunnel caused a forward movement of transition from laminar to turbulent heat transfer in clear air with a semilaminar region obtained at local Reynolds numbers of less than 10^6 .
3. The impingement of water on the airfoil model in both flight and in the icing-research tunnel caused a forward movement of transition. During the flight-icing conditions, only a very small region of laminar heat transfer resulted; no fully laminar heat transfer was obtained in the tunnel-icing investigations. Transition in the icing-research tunnel was initiated at local Reynolds numbers of from less than 3×10^5 to approximately 10^6 with full turbulent heat transfer being achieved at local Reynolds numbers varying from approximately 8×10^5 to 4×10^6 .

4. The type of heating and temperature patterns had measurable effects on the heat transfer.

5. The calculation of heating requirements based on the icing-research-tunnel convective-heat-transfer results will generally result in conservative values, that is more heat than necessary should be available to cope with the particular icing situation. The amount by which the heating requirements are conservative is dependent on the specific design conditions.

Lewis Flight Propulsion Laboratory
National Advisory Committee for Aeronautics
Cleveland, Ohio, April 6, 1951

APPENDIX - SYMBOLS

The following symbols are used in this report:

C	airfoil chord length, ft
c_p	specific heat of air at constant pressure, 0.24 Btu/(lb)(°F)
e	saturation vapor pressure, in. Hg
g	acceleration due to gravity, 32.2 ft/sec ²
h	heat-transfer coefficient, Btu/(hr)(sq ft)(°F)
J	mechanical equivalent of heat, 778 ft-lb/Btu
K	surface area wetted, percent
k	thermal conductivity of air, Btu/(hr)(sq ft)(°F)/(ft)
L	latent heat of vaporization of water assumed constant, 1090 Btu/lb
M_a	weight rate of water-droplet impingement per unit of surface area, lb/(hr)(sq ft)
n	exponent of Prandtl number: 1/2 for laminar flow; 1/3 for turbulent flow
N_{Nu}	Nusselt number ($h_c s/k$), dimensionless
N_{Pr}	Prandtl number ($3600 c_p \mu/k$), dimensionless
N_{Re}	Reynolds number ($V_0 C_r/\mu$), dimensionless, based on chord length and free-stream conditions
$N_{Re,s}$	Reynolds number ($U_{1s} r/\mu$), dimensionless, based on surface dis- tance and local surface conditions
p	static pressure, in. Hg
q	unit rate of heat flow, Btu/(hr)(sq ft)
s	distance measured chordwise along airfoil surface from stagna- tion point, ft

2175

t	temperature, °F
U	local velocity just outside boundary layer, ft/sec
V	true airspeed, ft/sec
X	Hardy's evaporation coefficient, dimensionless
γ	specific weight of air, lb/cu ft
μ	viscosity of air, lb/(sec)(ft)

Subscripts:

O	free stream
l	edge of boundary layer
a	surface datum with no heating or conduction
c	convective heat transfer
d	dry or clear air
e	evaporative heat transfer
m	sensible heat transfer
s	airfoil surface
T	total or static plus dynamic
w	wet air or cloud

Superscript:

'	dry air
---	---------

REFERENCES

1. Jones, Alun R., and Rodert, Lewis A.: Development of Thermal Ice-Prevention Equipment for the B-24D Airplane. NACA ACR, Feb. 1943.
2. Hardy, J. K.: Protection of Aircraft against Ice. Rep. No. S.M.E. 3380, British R.A.E., July 1946.
3. Neel, Carr B., Jr., Bergrun, Norman R., Jukoff, David, and Schlaff, Bernard A.: The Calculation of the Heat Required for Wing Thermal Ice Prevention in Specified Icing Conditions. NACA TN 1472, 1947.
4. Anon.: The Multicylinder Method. The Mount Washington Monthly Res. Bull., vol. II, no. 6, June 1946.
5. Hardy, J. K.: An Analysis of the Dissipation of Heat in Conditions of Icing from a Section of the Wing of the C-46 Airplane. NACA Rep. 831, 1945. (Formerly NACA ARR 4111a.)
6. Boelter, L. M. K., Grossman, L. M., Martinelli, R. C., and Morrin, E. H.: An Investigation of Aircraft Heaters. XXIX - Comparison of Several Methods of Calculating Heat Losses from Airfoils. NACA TN 1453, 1948.
7. Eckert, E., and Drewitz, O.: Calculation of the Temperature Field in the Laminar Boundary Layer of an Unheated Body in a High Speed Gas Flow. R.T.P. Trans. No. 1594, British M.A.P.

TABLE I - OPERATING CONDITIONS FOR FLIGHT AND ICING-RESEARCH TUNNEL INVESTIGATIONS
OF NACA 65,2-016 ELECTRICALLY HEATED AIRFOIL MODEL

[Spray 48 ft upstream of model except when noted.]



Condition	True air- speed (mph)	Free- stream tempera- ture (°F)	Free-stream Reynolds number	Liquid- water content (g/cu m)	Mean- effective droplet diameter (microns)	Droplet- size distri- bution	Remarks
a ₁	167	19	9.65 × 10 ⁶	0.26	13	D	Flight icing, condition 1
a ₂	168	26	1.24	0.34	18	E	Flight icing, condition 2
a ₃	157	19	11.25	0.44	13	B	Flight icing, condition 3
a ₄	158	21	11.29	0.42	19	D	Flight icing, condition 5
a ₅ ^a	145	38	9.65	0	--	-	Flight in clear air
6	156	14	13.10	0.7	9	F	Tunnel, simulation of flight
6'	156	14	13.10	0	--	-	Tunnel, simulation of flight
7	168	11	14.25	0.4	10	D	Tunnel, simulation of flight
7'	168	11	14.25	0	--	-	Tunnel, simulation of flight
8	165	21	13.49	0.5	11	E	Tunnel, simulation of flight
8'	165	21	13.49	0	--	-	Tunnel, simulation of flight
9	159	13	13.40	1.2	10	D	Tunnel, simulation of flight
9'	159	13	13.40	0	--	-	Tunnel, simulation of flight
10	200	12	16.45	0.9	12	E	Tunnel, uniform surface temperature
10'	200	12	16.45	0	--	-	Tunnel, nonuniform surface temperature
11	193	9	16.20	0.55	12	E	Tunnel, nonuniform surface temperature
11'	193	9	16.20	0	--	-	Tunnel, uniform surface temperature
12'	138	18	11.45	0	--	-	Tunnel, uniform surface temperature; spray out
13'	194	11	16.08	0	--	-	Tunnel, uniform surface temperature; spray out
14'	133	16	11.0	0	--	-	Tunnel, uniform surface temperature; spray at 22 feet

^aData from reference 3.

TABLE II - VALUES OF CALCULATED WATER-DROPLET IMPINGEMENT OVER LEADING EDGE OF
ELECTRICALLY HEATED AIRFOIL MODEL FOR CONDITIONS OF TABLE I

[Based on water-droplet trajectories for symmetrical,
12-percent-thick Joukowski airfoil.]



Condition	Calculated rate of water-droplet impingement per foot of span for one side of airfoil (lb/(hr)(ft span))	Calculated limit of water droplet impingement, s/C (percent)	Calculated rate of water evaporated in impinged area per foot of span for one side of airfoil (lb/(hr)(ft span))	Calculated limit of runback of water, s/C (percent)
1	0.3	2.9	0.2	19
2	.85	6.5	.3	35
3	.35	1.6	.1	32
4	.95	5.0	.2	40
6	.5	2.9	.2	38
7	.25	2.0	.1	34
8	.5	3.0	.25	32
9	.75	2.0	.1	32
10	2.5	4.0	.1	55
11	.9	3.6	.15	34

^a Runback ice forms beginning in this region.

2175

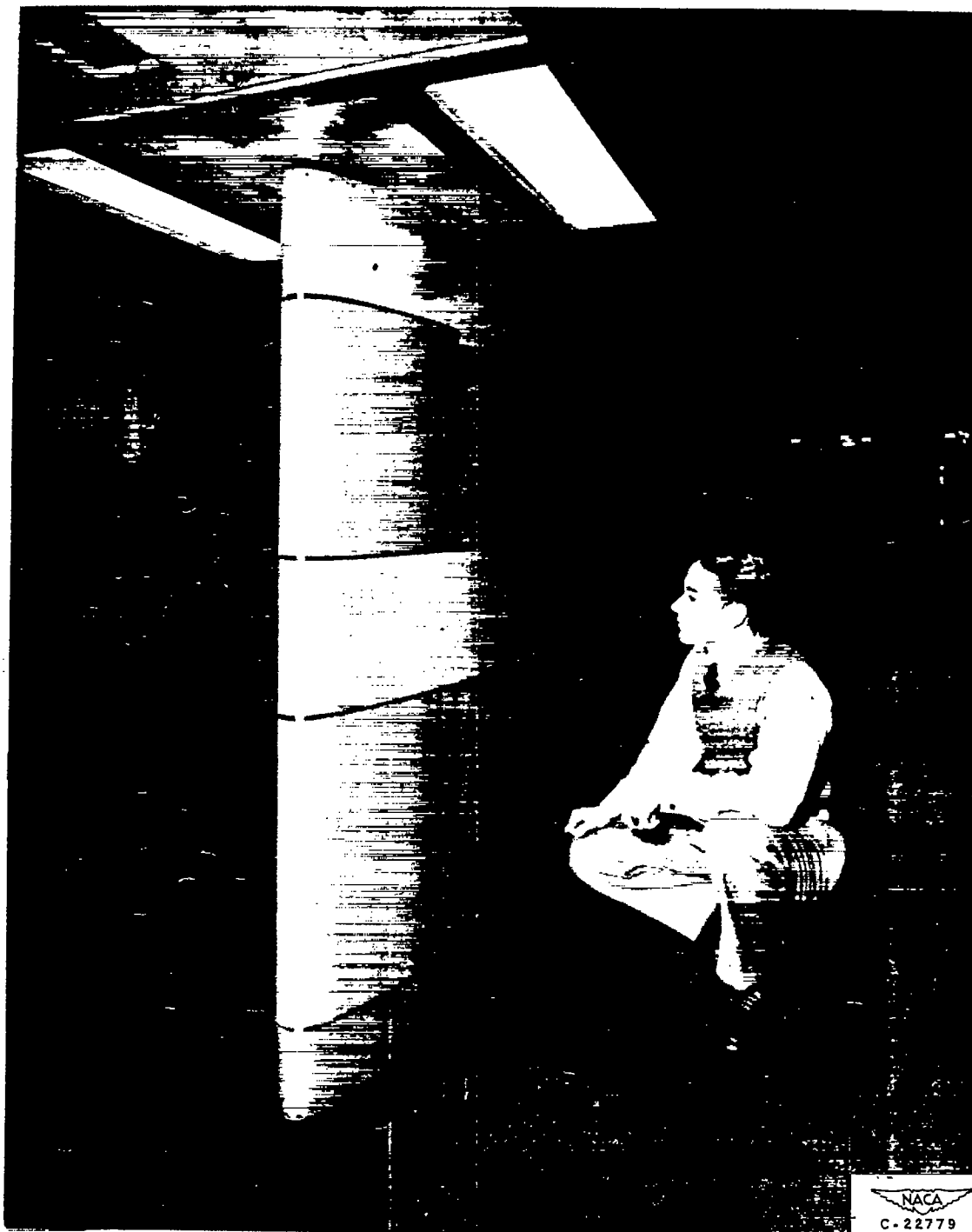


Figure 1. - Installation of NACA 65,2-016 electrically heated airfoil model in test section of icing-tunnel.

NACA
C-22779

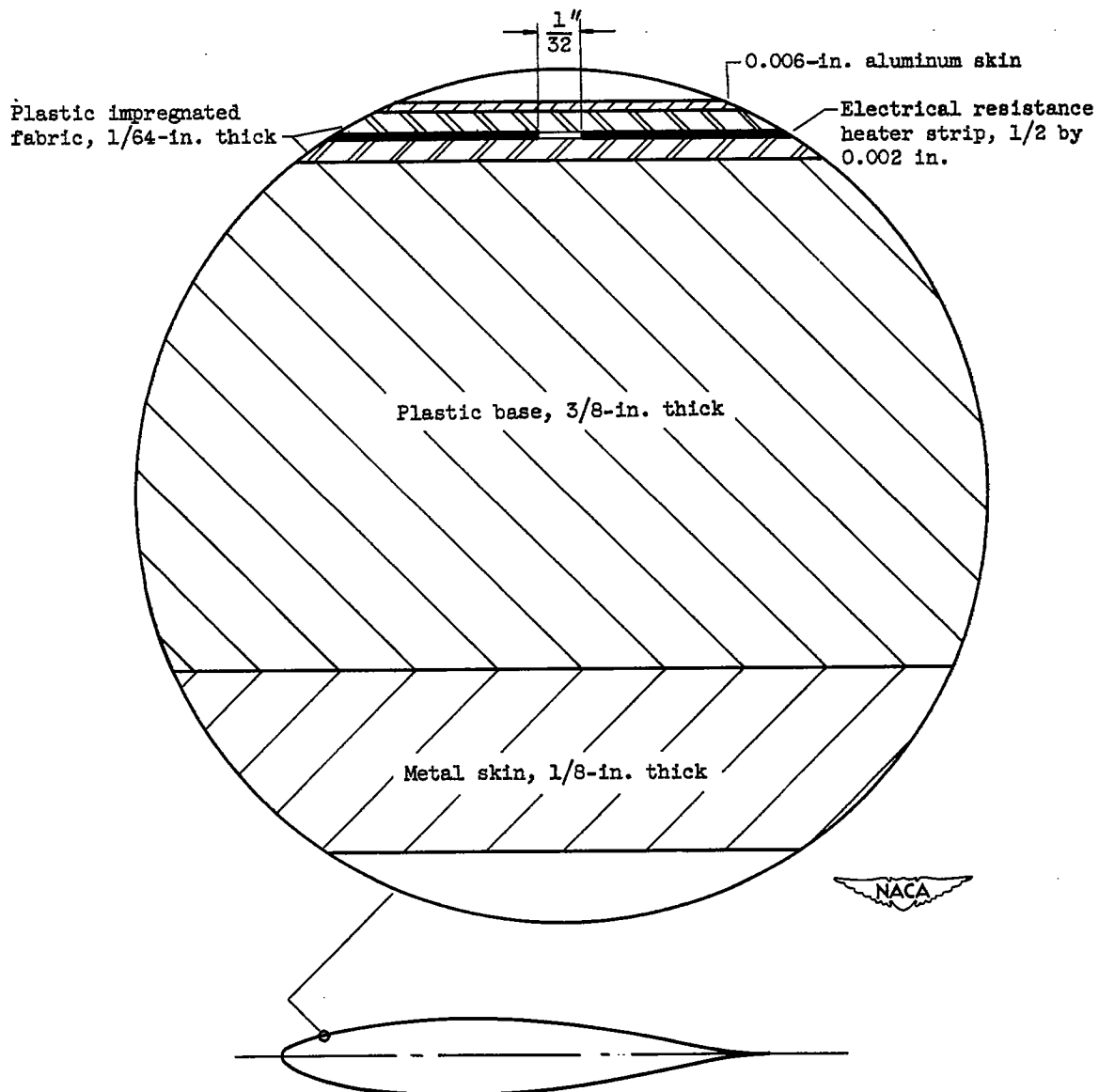


Figure 2. - Schematic diagram showing construction details of test section of NACA 65,2-016 electrically heated airfoil model.

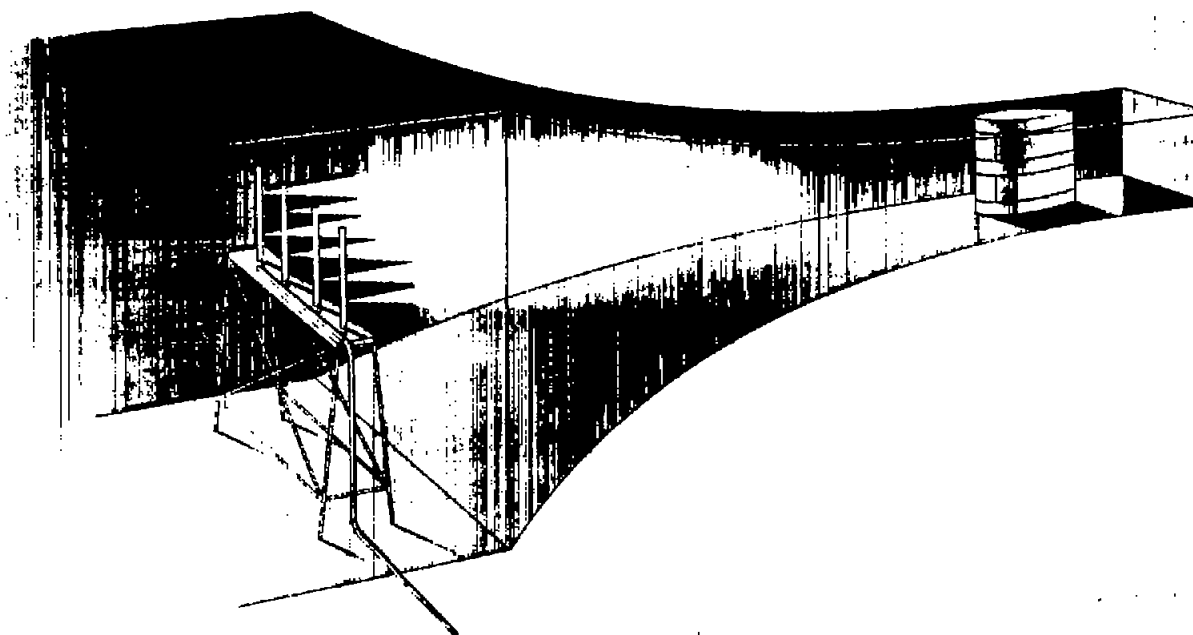


Figure 3. - Water spray system and airfoil model installed in icing-tunnel. Spray system, 48 feet upstream of model.

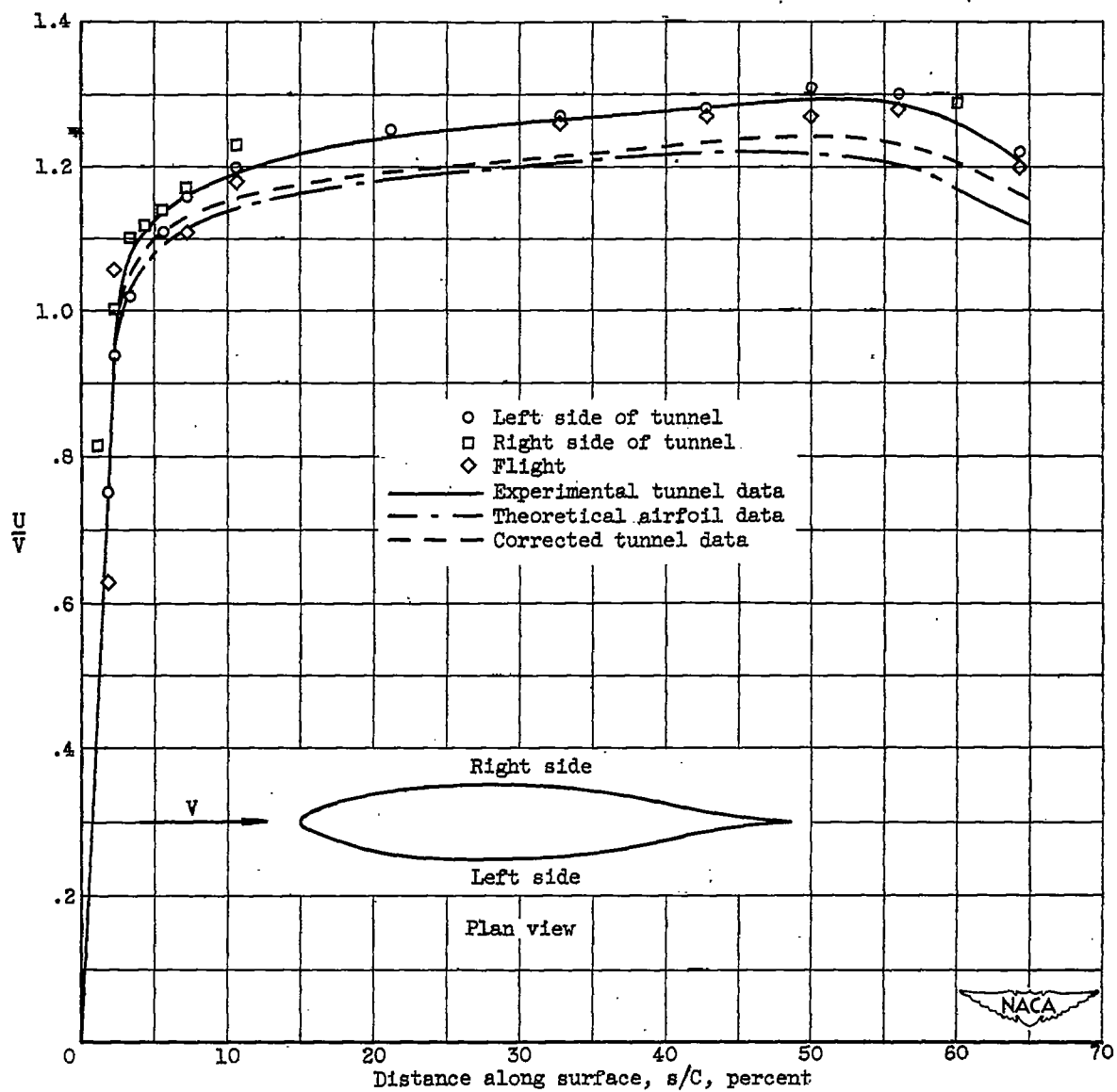


Figure 4. - Velocity distribution over NACA 65,2-016 electrically heated airfoil model. Angle of attack, 0° ; average Reynolds number N_{Re} , 12×10^6 .

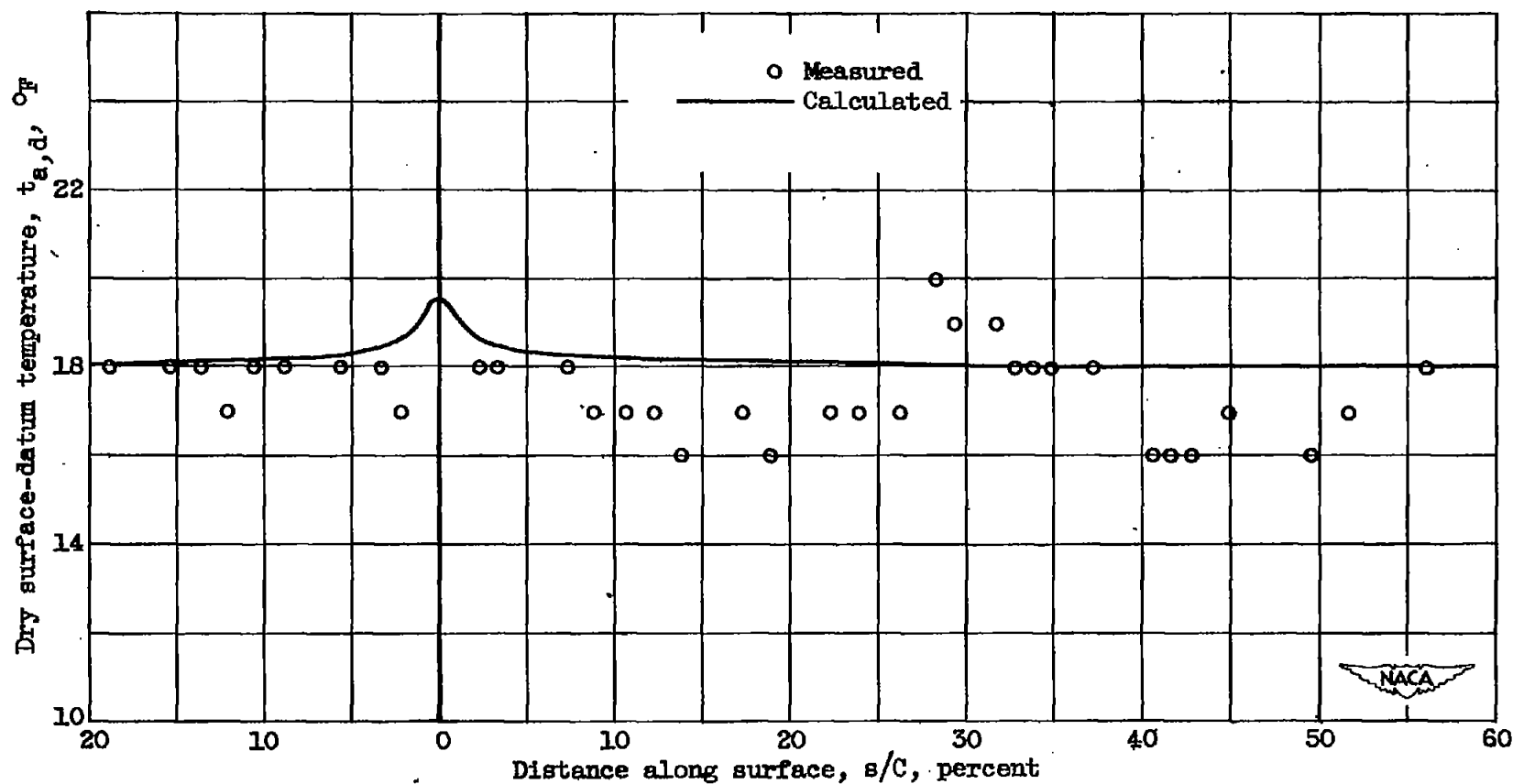
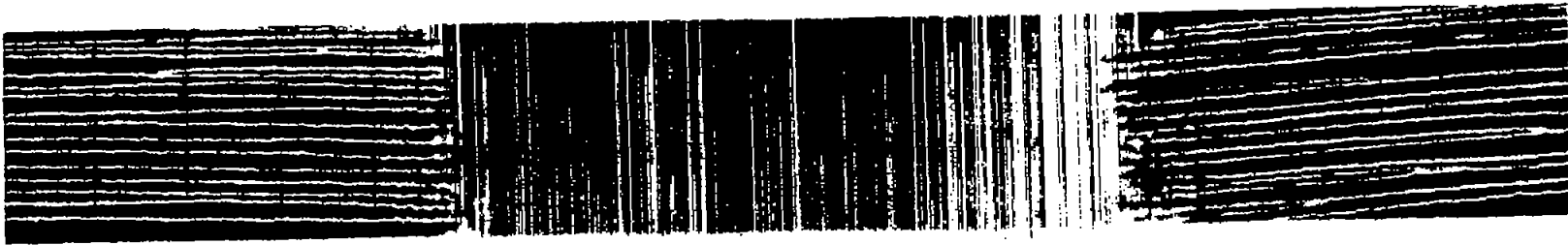
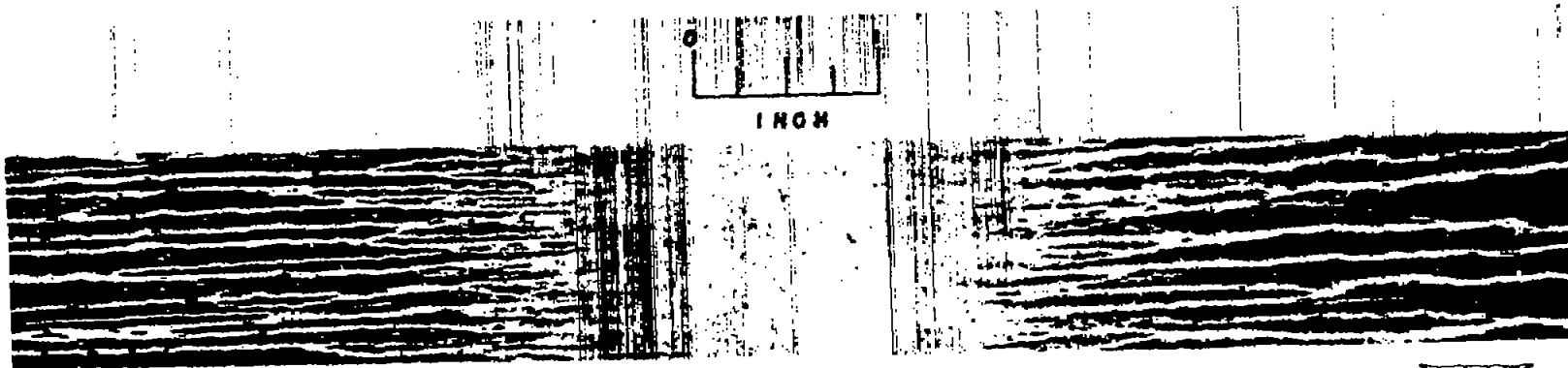


Figure 5. - Comparison of measured with calculated surface-datum temperatures for condition 10'. Icing tunnel clear-air investigation, spray system 48 feet upstream of NACA 65,2-016 electrically heated airfoil model. Free-stream temperature, 12° F.



(a) Flight record.



(b) Icing-tunnel record.

NACA
C-26520

Figure 6. - Typical records of water-droplet impingement and runback on NACA 65,2-016 airfoil model in flight and in icing-tunnel.

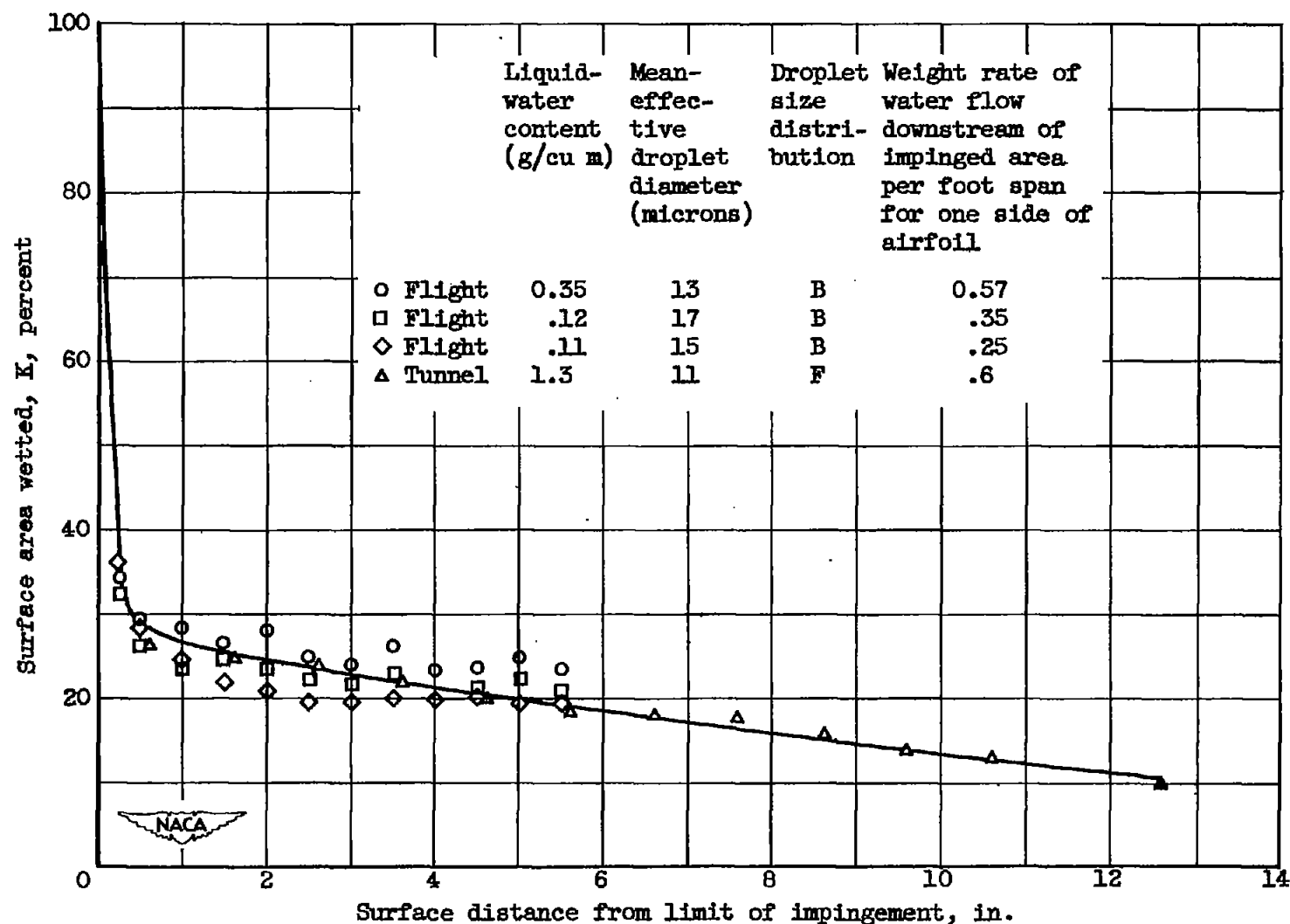


Figure 7. - Measured percentage of surface area wetted in runback region for three flight and one icing tunnel investigation on NACA 65,2-016 airfoil model.

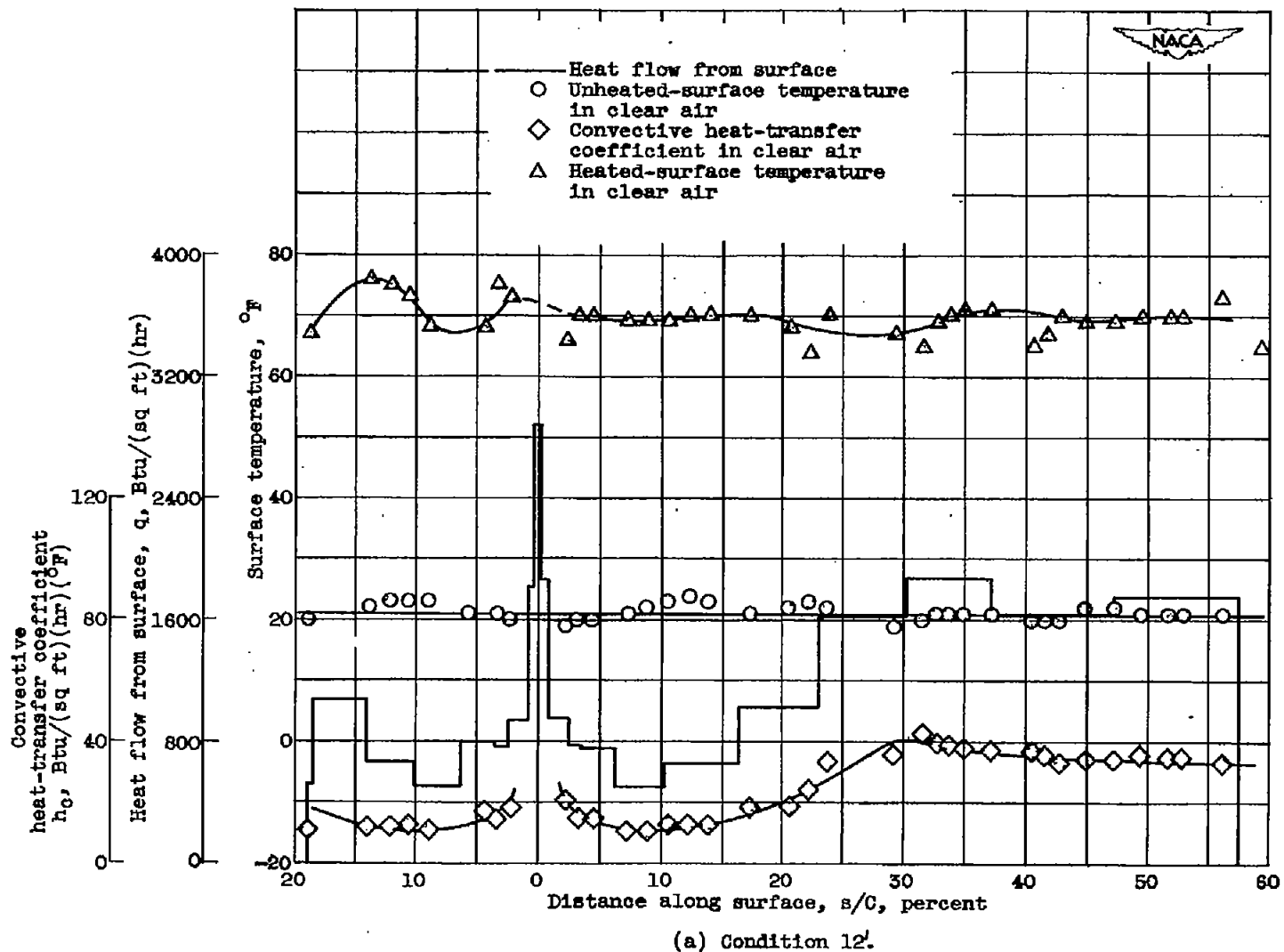


Figure 8. - Thermal data obtained in clear air in tunnel. Tunnel heating distribution on NACA 65,2-016 electrically heated airfoil model; spray system removed from tunnel.

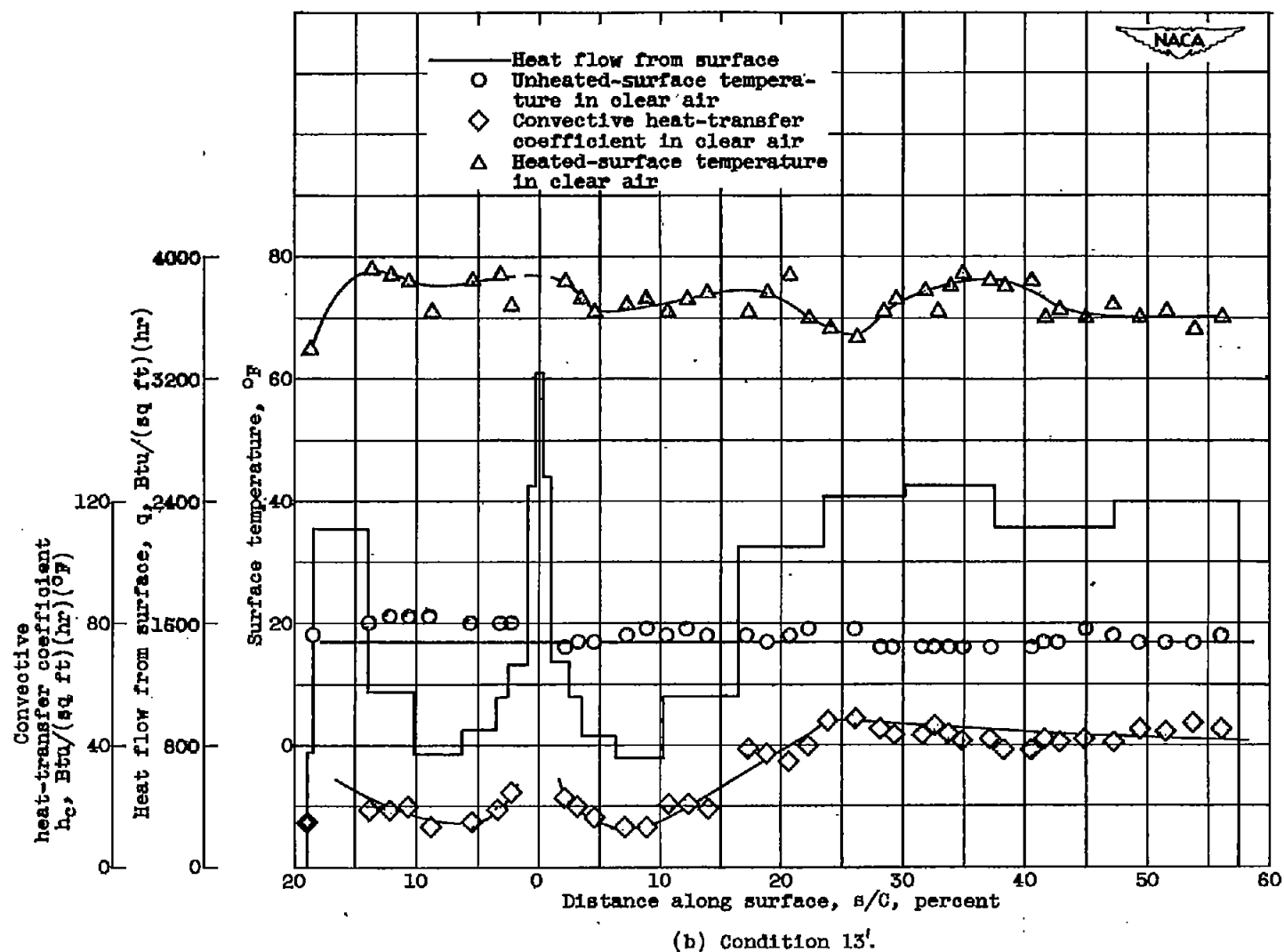
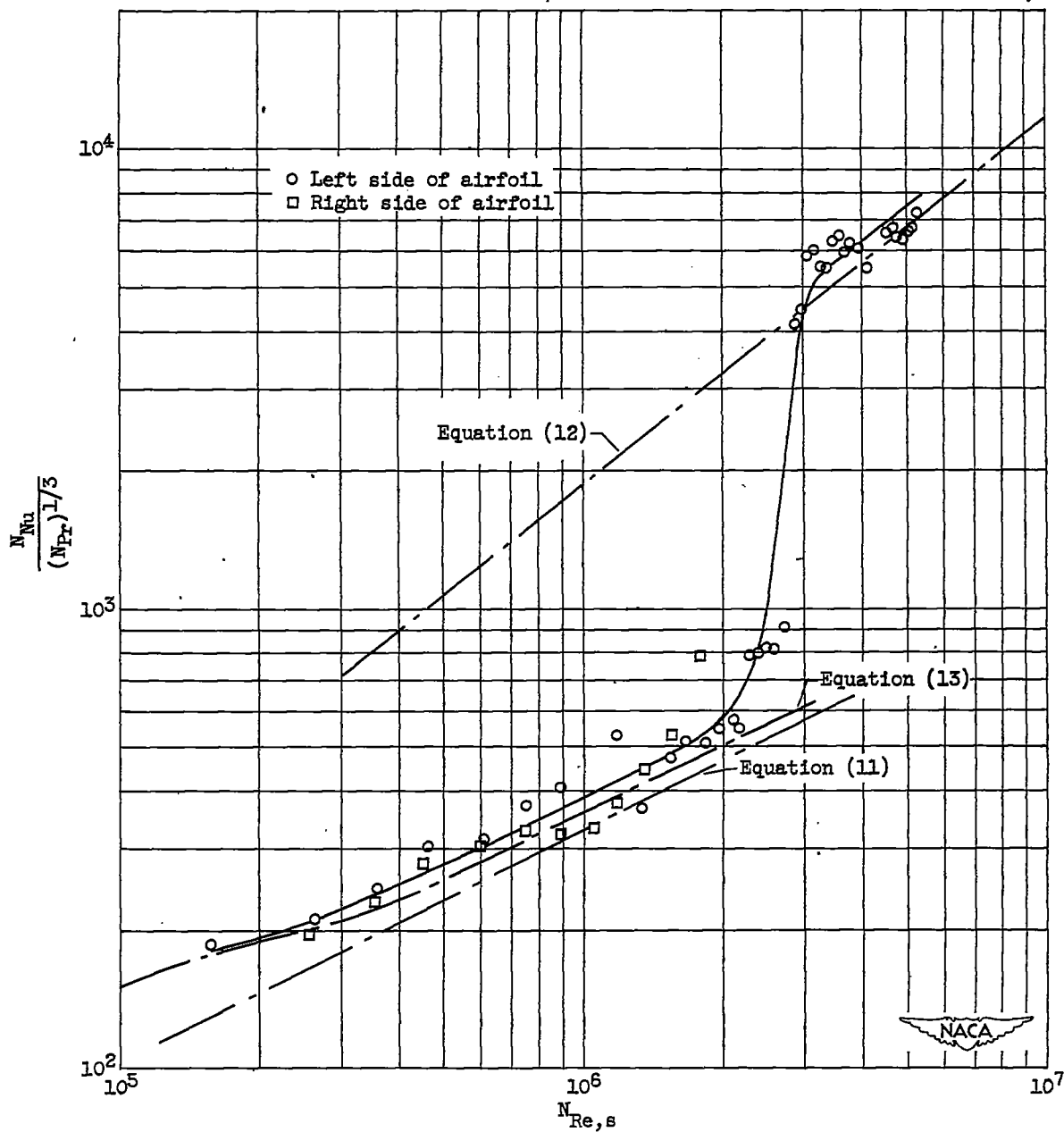
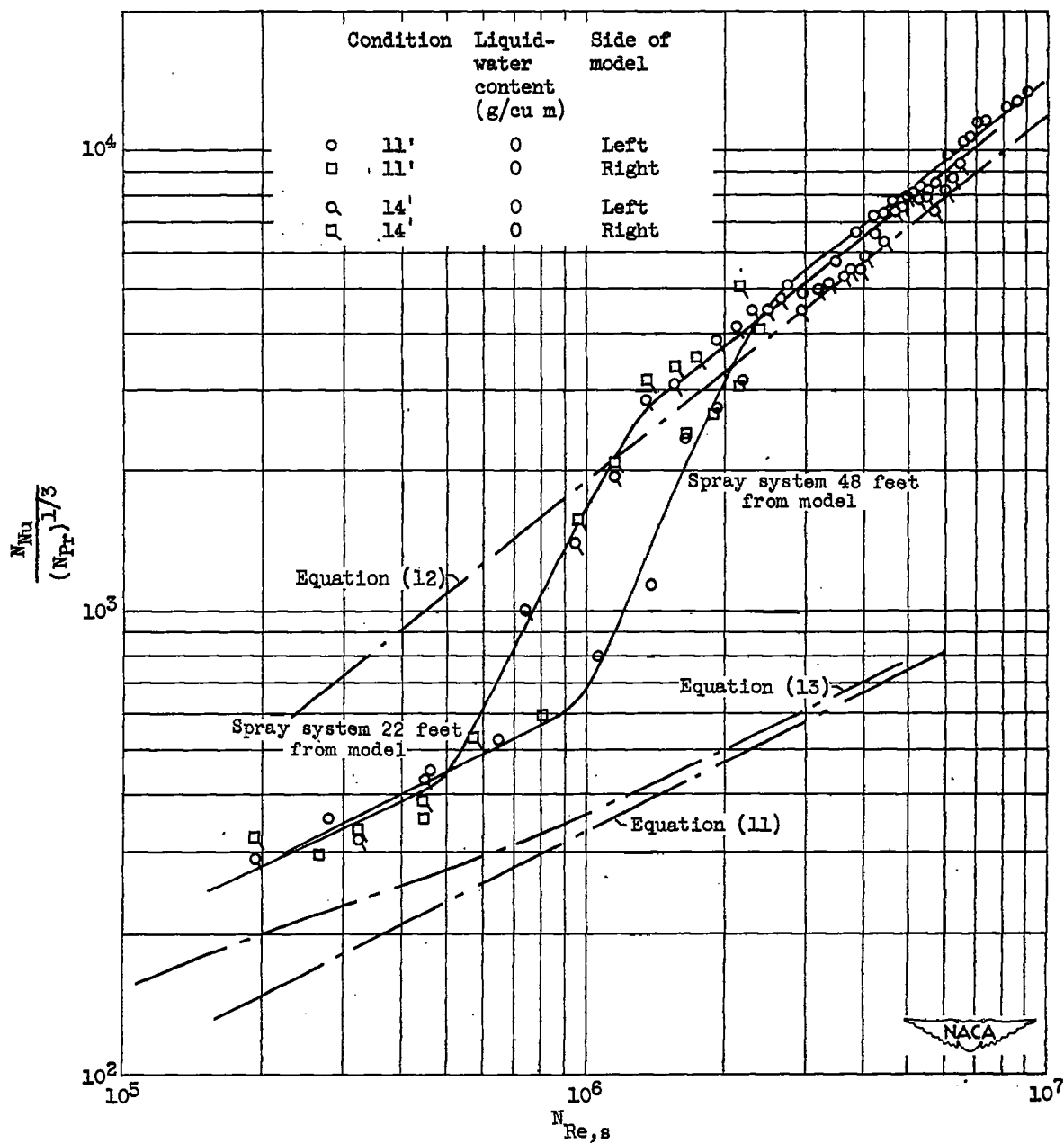


Figure 8. - Concluded. Thermal data obtained in clear air in tunnel. Tunnel heating distribution on NACA 65,2-016 electrically heated airfoil model; spray system removed from tunnel.



(b) Condition 5'.

Figure 9. - Continued. Correlation of heat-transfer data. Heating distribution resulting in uniform surface temperatures.



(c) Conditions 11' and 14'.

Figure 9. - Concluded. Correlation of heat-transfer data. Heating distribution resulting in uniform surface temperatures.

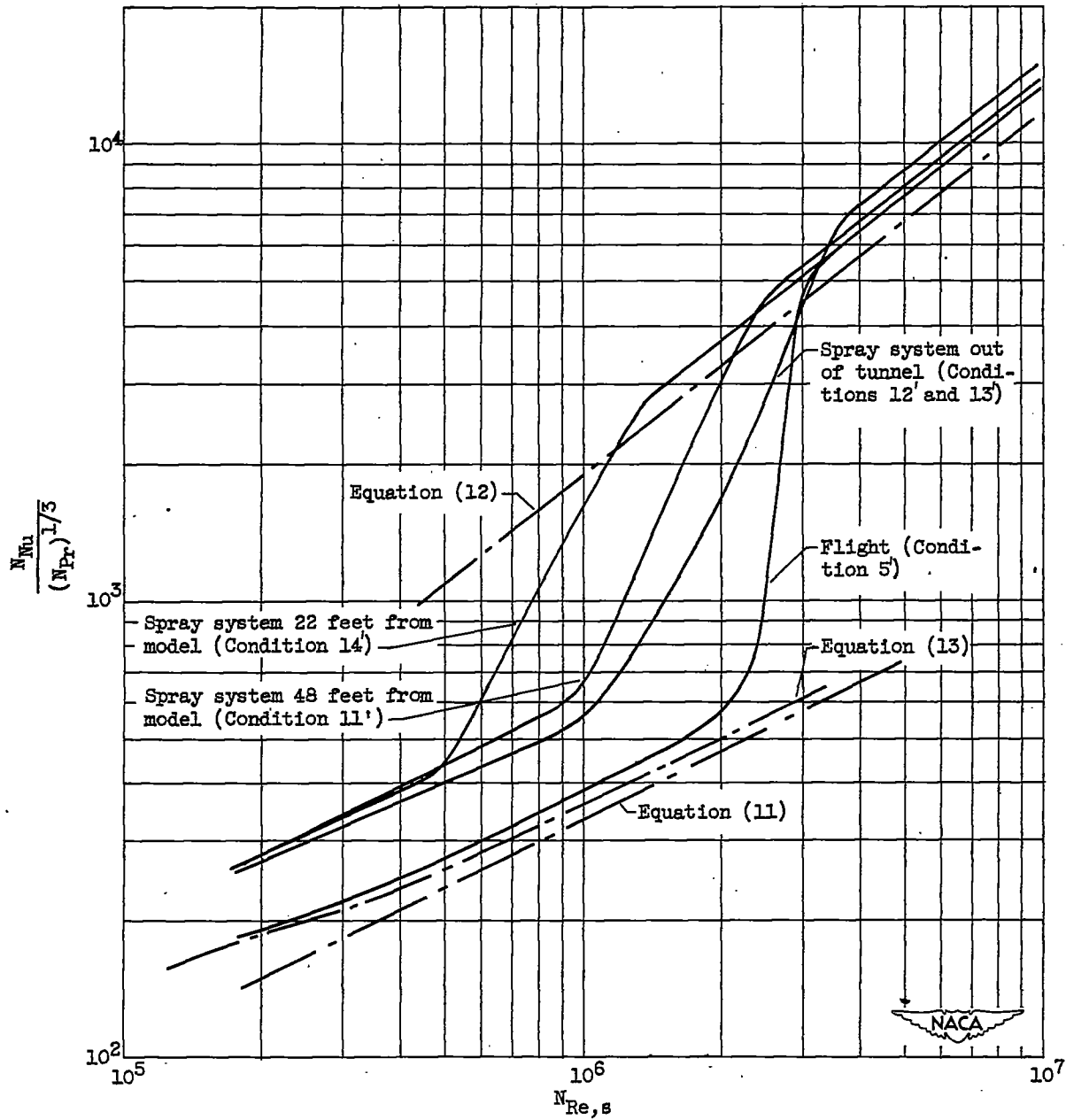


Figure 10. - Comparison of heat-transfer characteristics of four tunnel and one flight investigation. Uniform surface temperatures in clear air. Conditions 5', 11', 12', 13', and 14'.

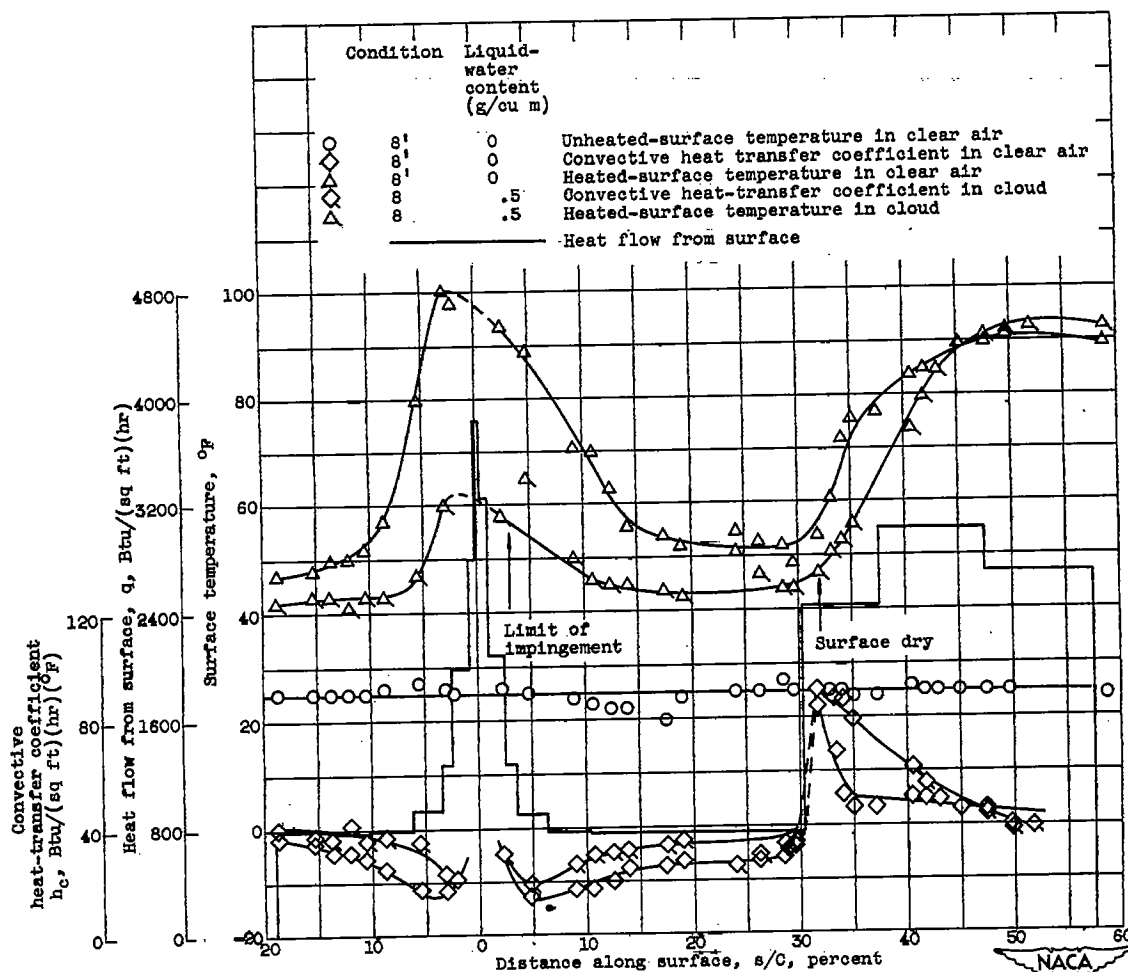
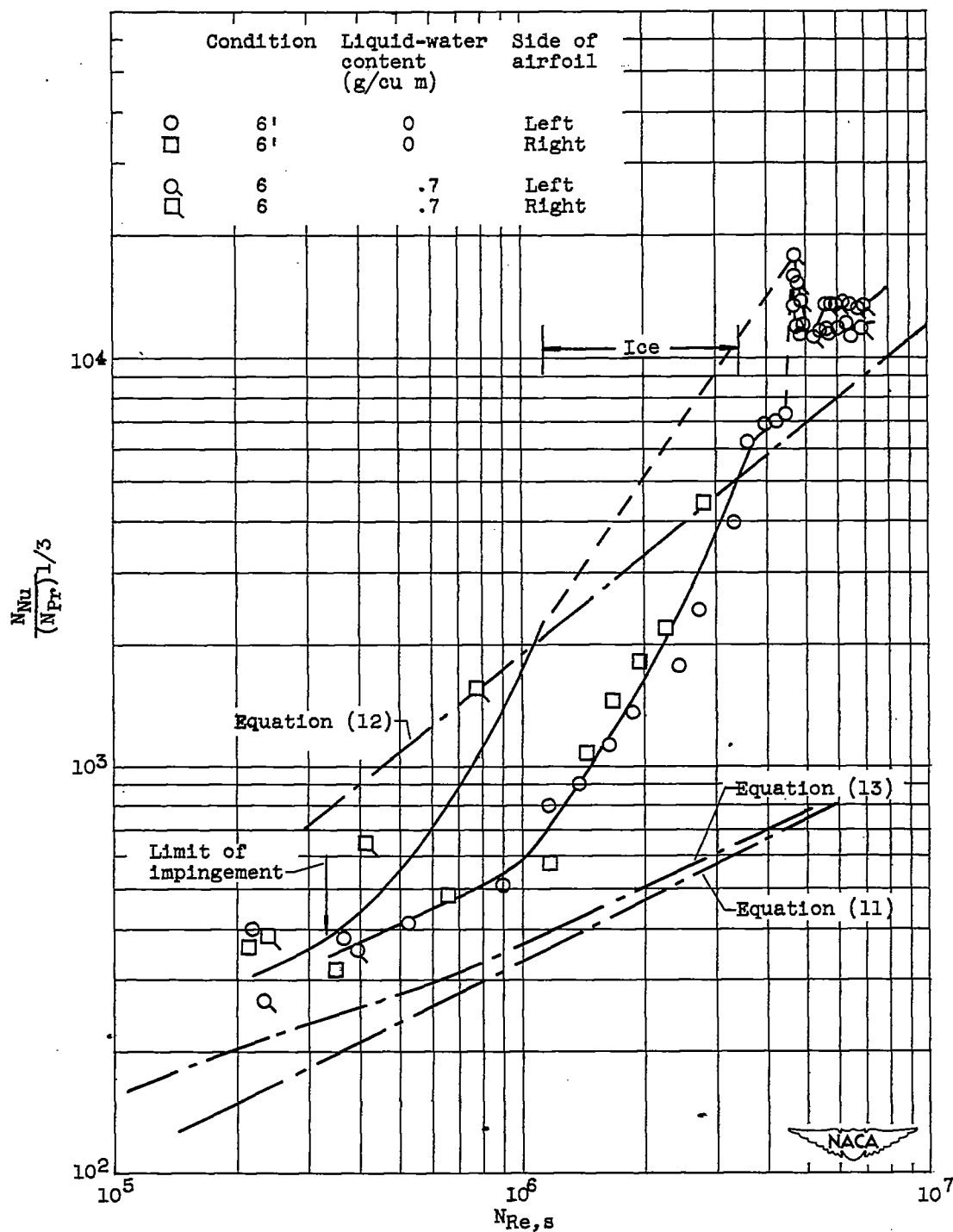
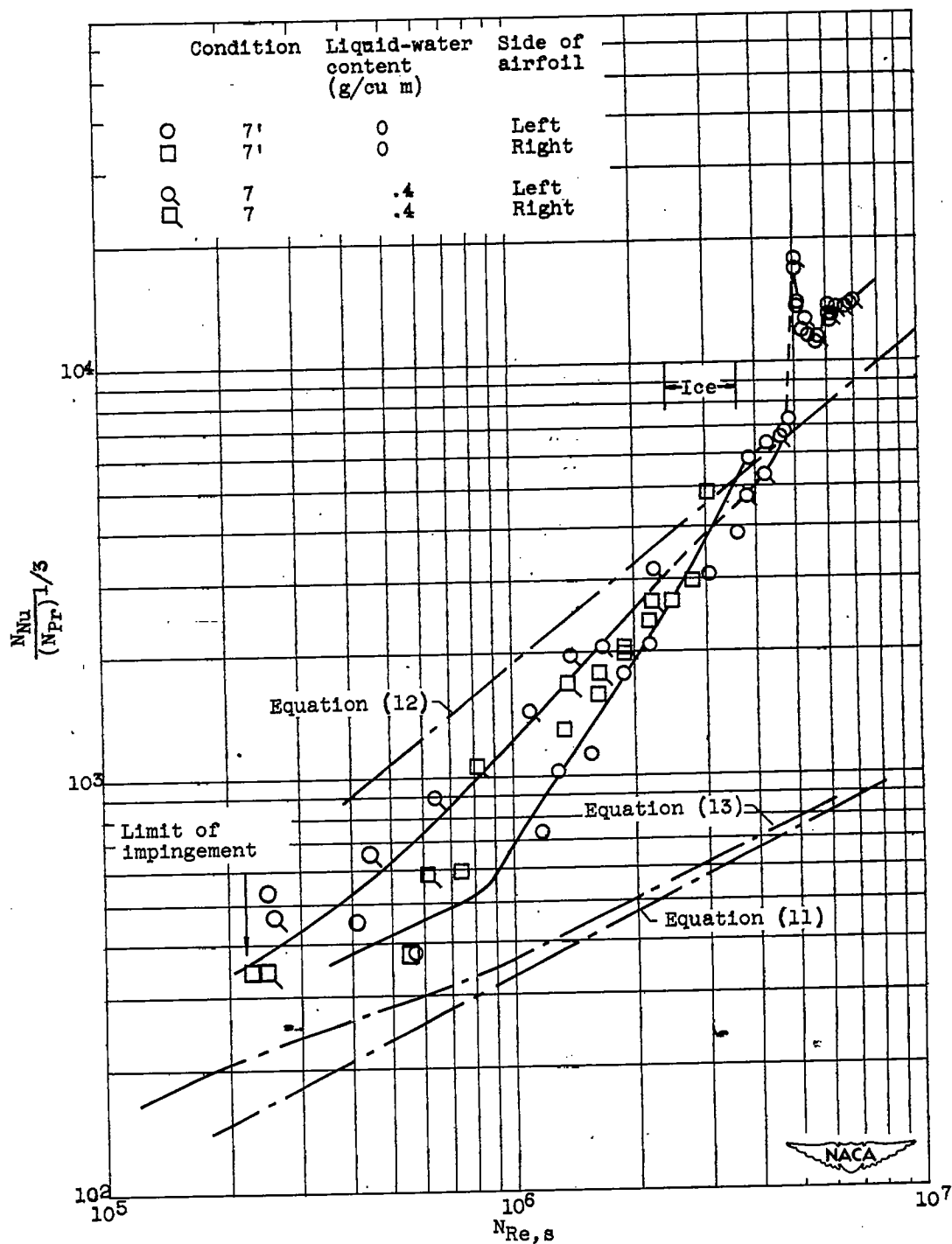


Figure 11. - Thermal data obtained in clear air and in icing in icing-research tunnel. Simulation of flight heating distribution. Spray system 48 feet upstream of NACA 65,2-016 electrically heated airfoil model. Conditions 8 and 8'.



(a) Conditions 6' and 6.

Figure 12. - Correlation of heat-transfer data obtained in clear air and in icing in icing-research tunnel. Simulation of flight heating distribution resulting in nonuniform surface temperature; spray system 48 feet upstream of model.



(b) Conditions 7' and 7.

Figure 12. - Continued. Correlation of heat-transfer data obtained in clear air and in icing in icing-research tunnel. Simulation of flight heating distribution resulting in nonuniform surface temperatures; spray system 48 feet upstream of model.

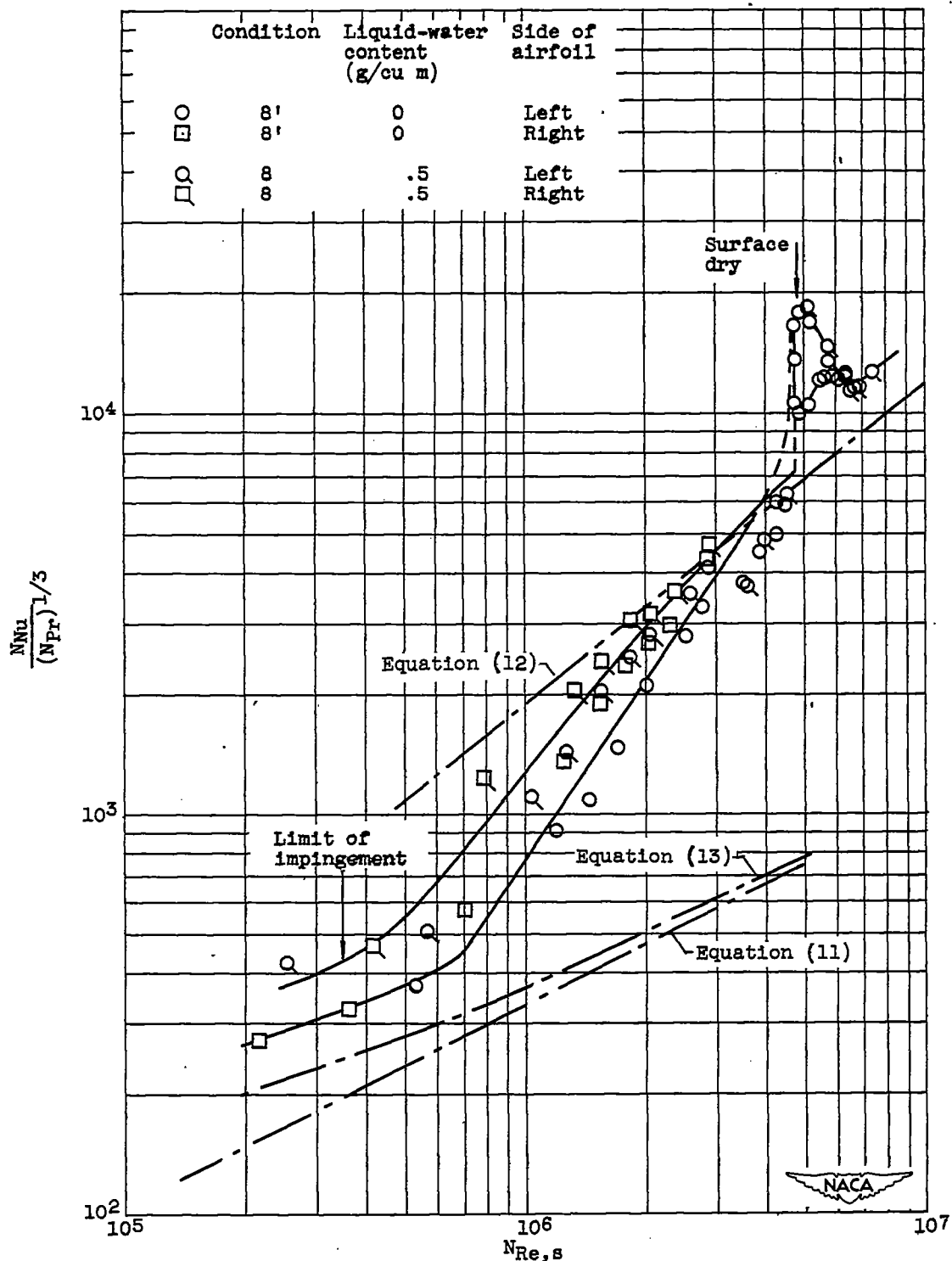
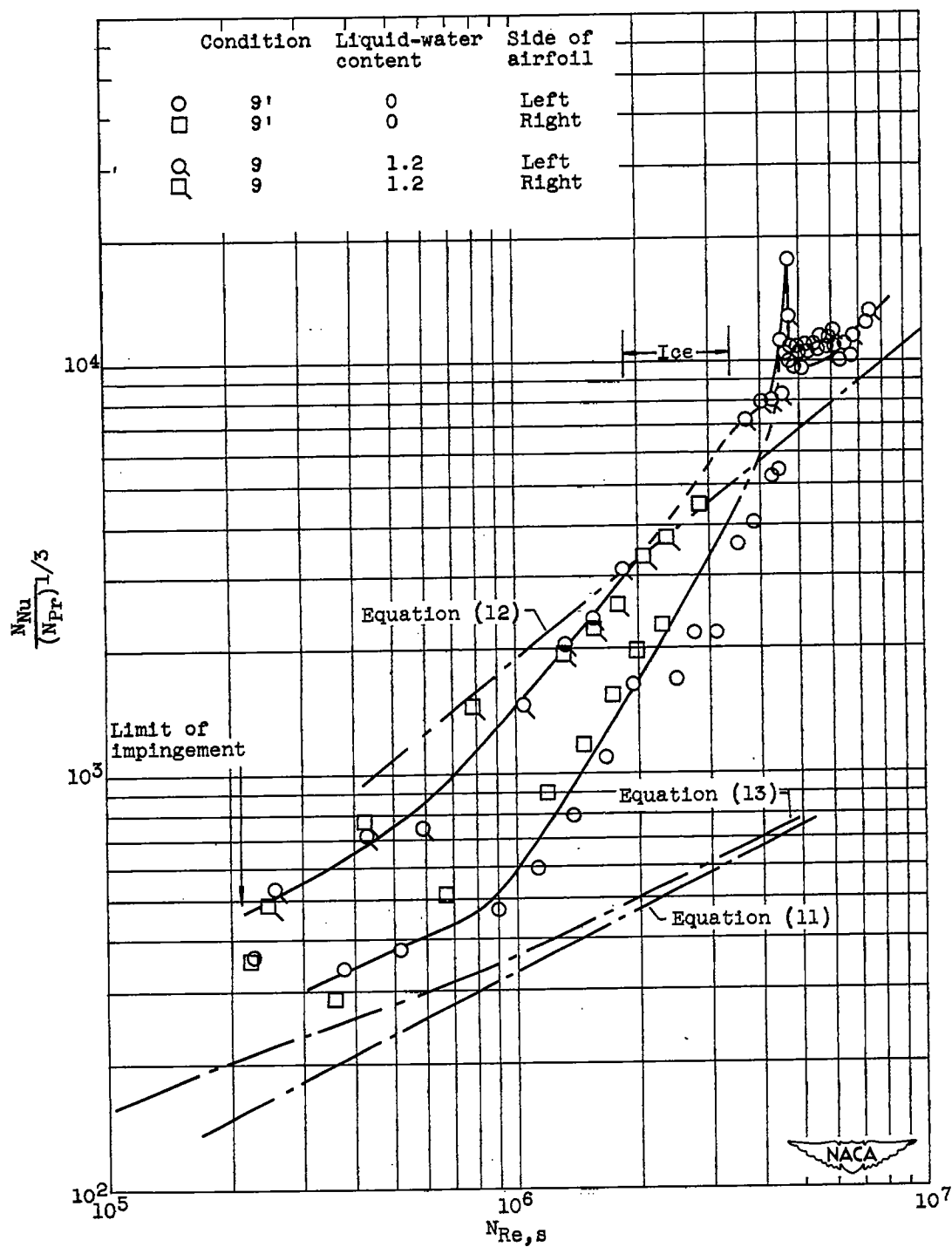


Figure 12. - Continued. Correlation of heat-transfer data obtained in clear air and in icing in icing-research tunnel. Simulation of flight heating distribution resulting in nonuniform surface temperatures; spray system 48 feet upstream of model.

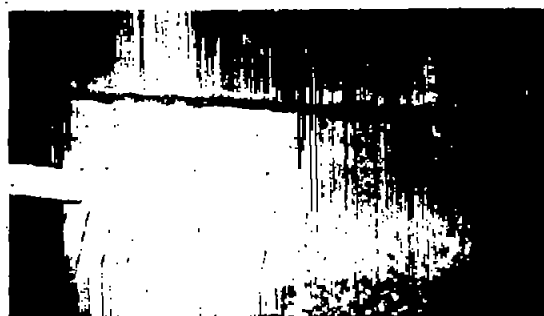


(d) Conditions 9' and 9.

Figure 12. - Concluded. Correlation of heat-transfer data obtained in clear air and in icing in icing-research tunnel. Simulation of flight heating distribution resulting in nonuniform surface temperatures; spray system 48 feet upstream of model.



(a) Condition 6.

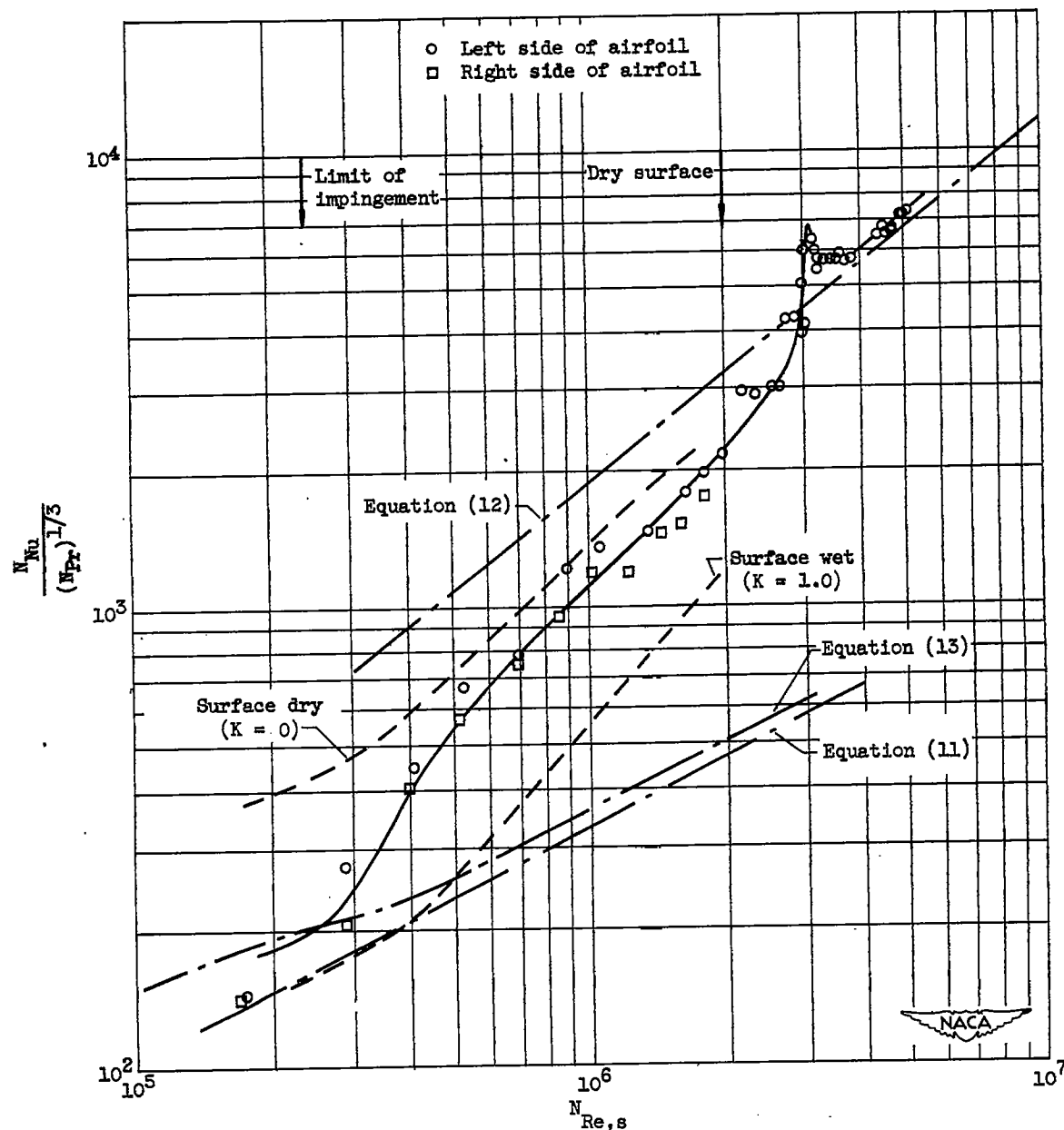


(b) Condition 9.

Left side of airfoil

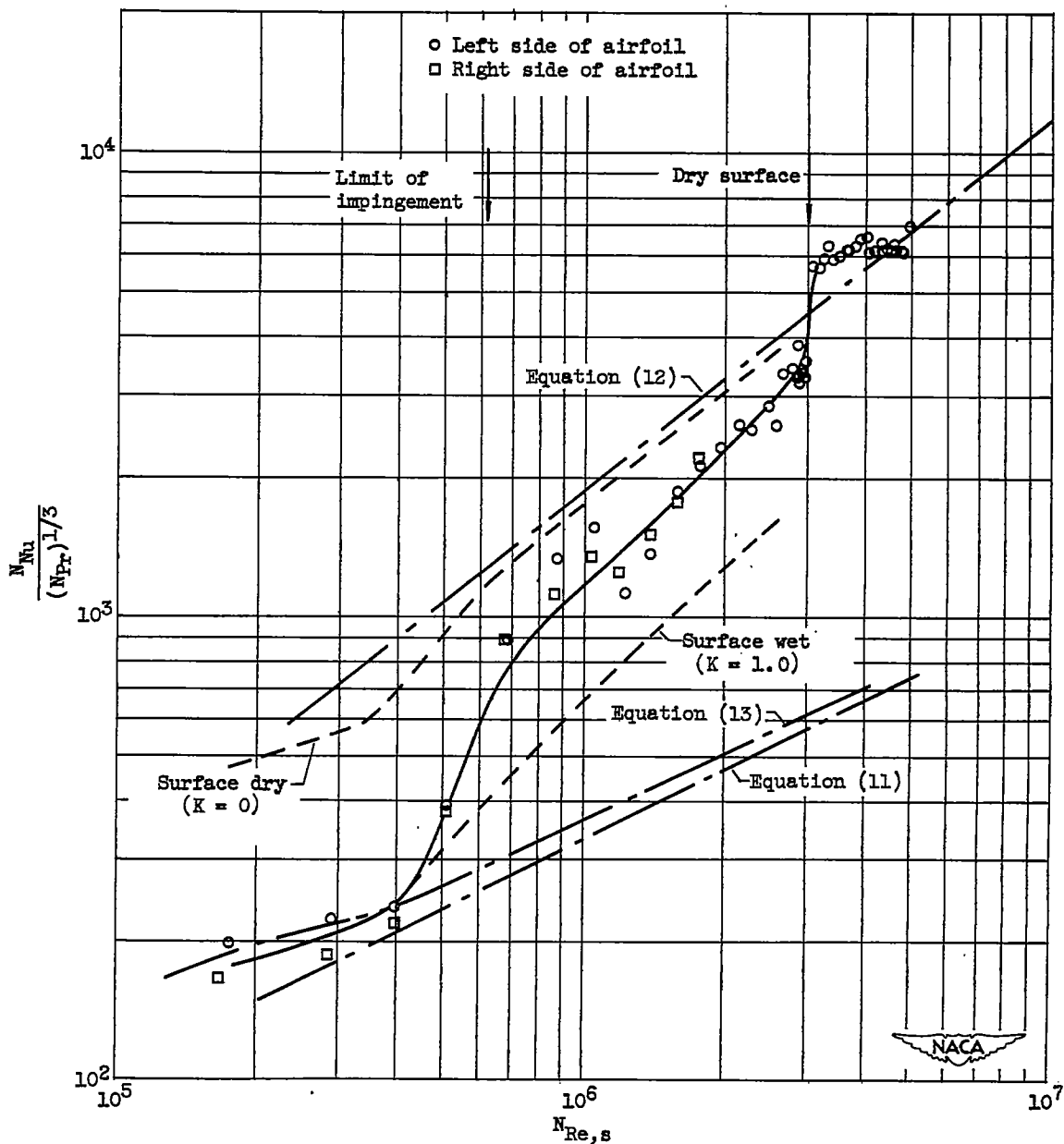
Right side of airfoil

Figure 13. - Ice formations on NACA 65,2-016 electrically heated airfoil model in icing-tunnel.



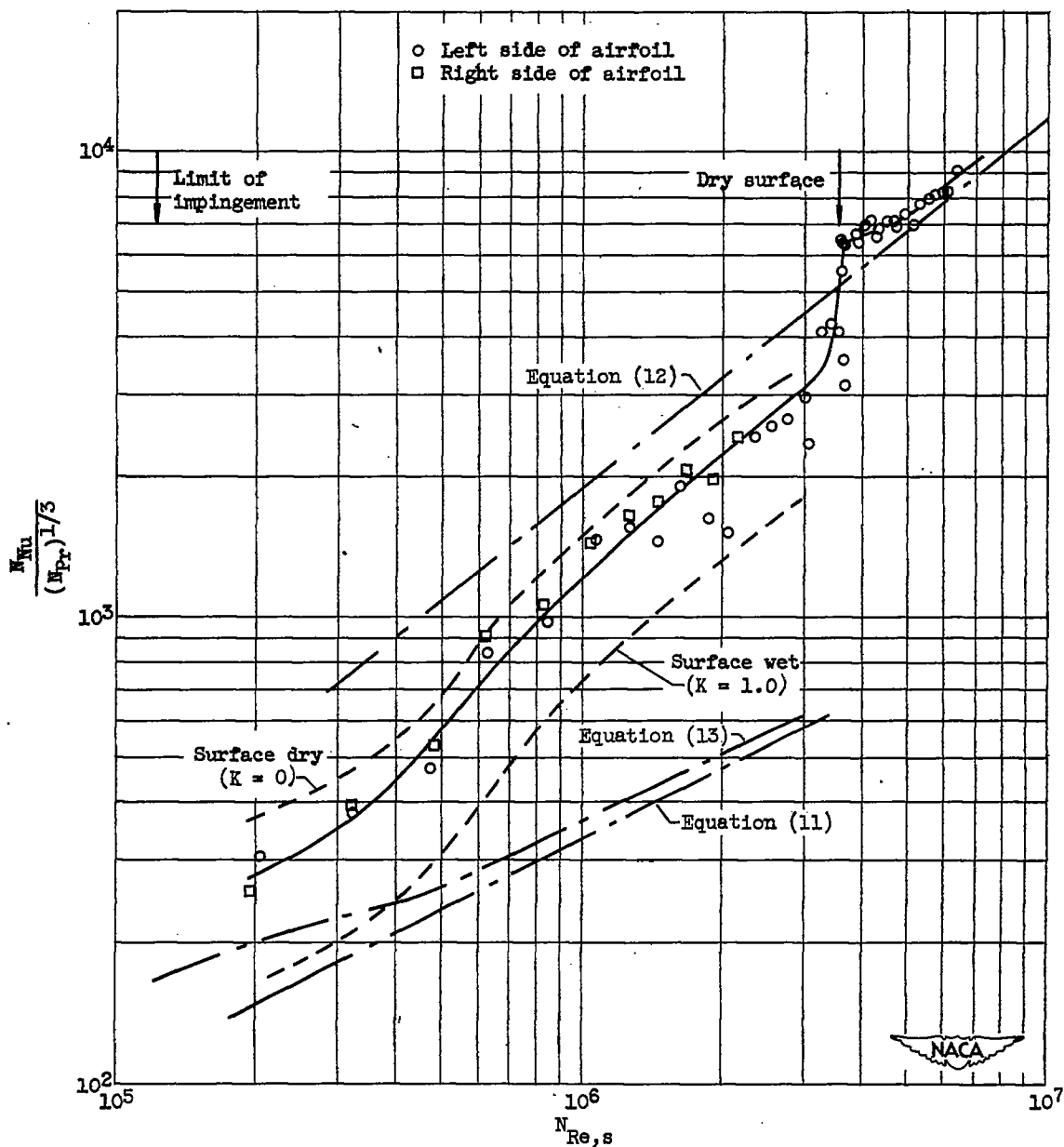
(a) Condition 1.

Figure 14. - Correlation of heat-transfer data obtained in flight investigation (reference 3). Heating distribution resulting in uniform surface temperatures in clear air but nonuniform surface temperatures in icing; NACA 65,2-016 electrically heated airfoil model.



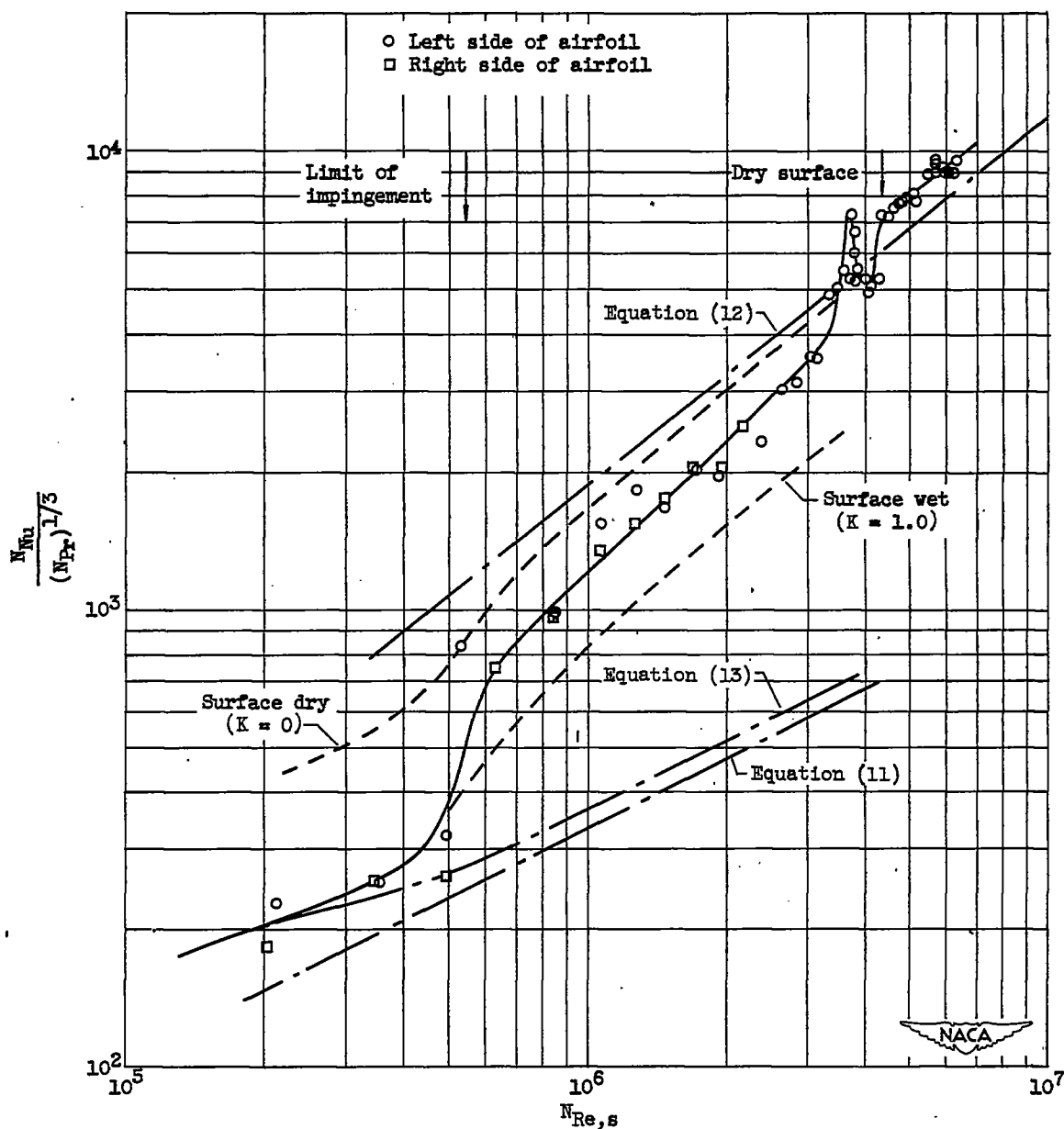
(b) Condition 2.

Figure 14. - Continued. Correlation of heat-transfer data obtained in flight investigation (reference 3). Heating distribution resulting in uniform surface temperatures in clear air but nonuniform surface temperatures in icing; NACA 65,2-016 electrically heated airfoil model.



(c) Condition 3.

Figure 14. - Continued. Correlation of heat-transfer data obtained in flight investigation (reference 3). Heating distribution resulting in uniform surface temperatures in clear air but nonuniform surface temperatures in icing; NACA 65,2-016 electrically heated airfoil model.



(d) Condition 4.

Figure 14. - Concluded. Correlation of heat-transfer data obtained in flight investigation (reference 3). Heating distribution resulting in uniform surface temperatures in clear air but nonuniform surface temperatures in icing; NACA 65,2-016 electrically heated airfoil model.

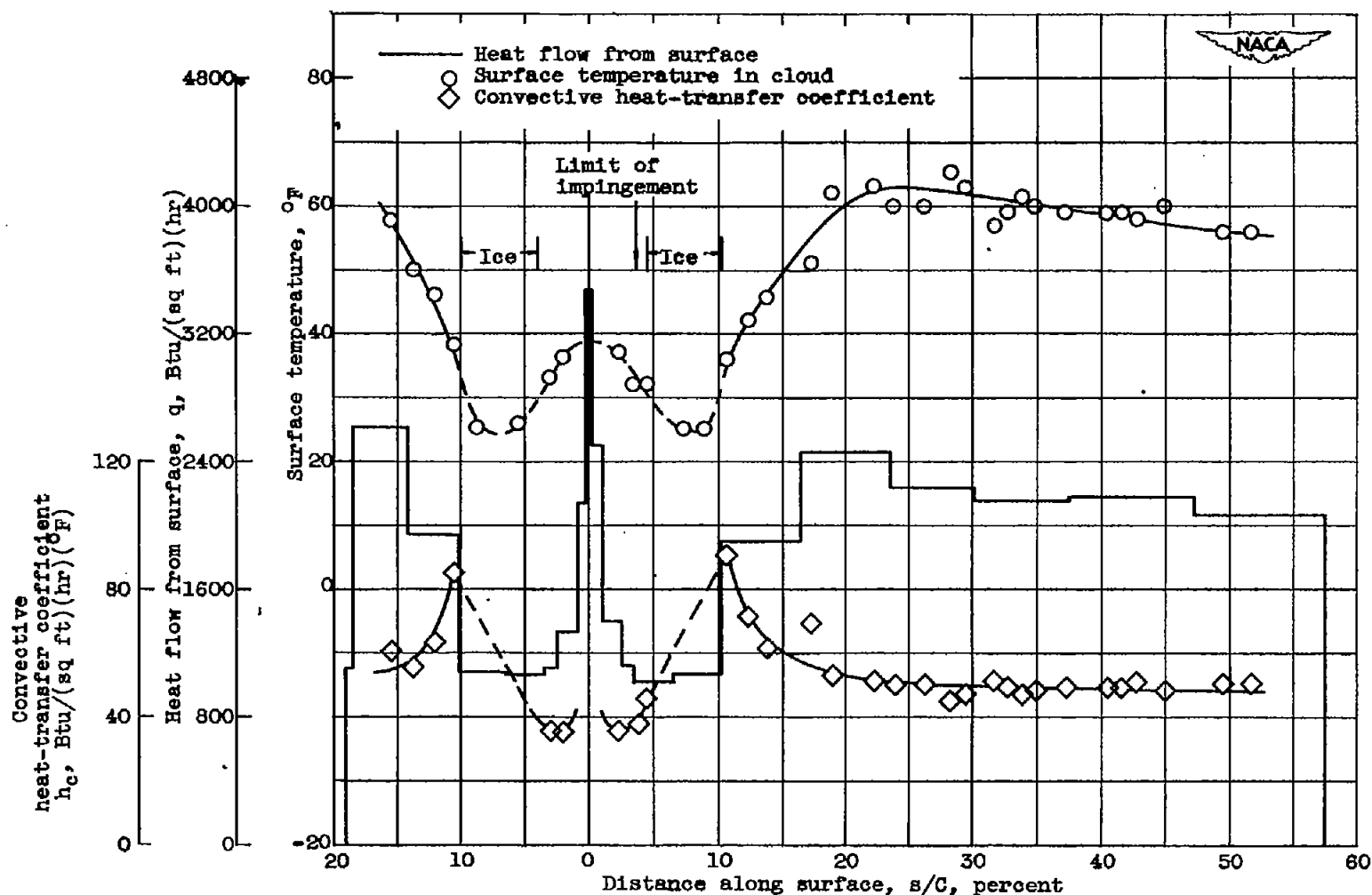
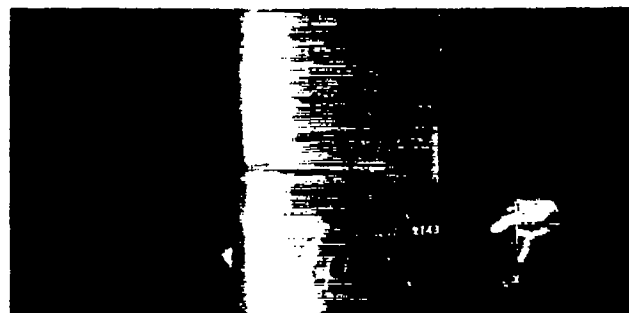


Figure 15. - Thermal data obtained in icing in icing-research tunnel. Tunnel heating distribution resulting in uniform surface temperatures in clear air; spray system 48 feet upstream of NACA 65,2-016 electrically heated airfoil model; condition 11'.



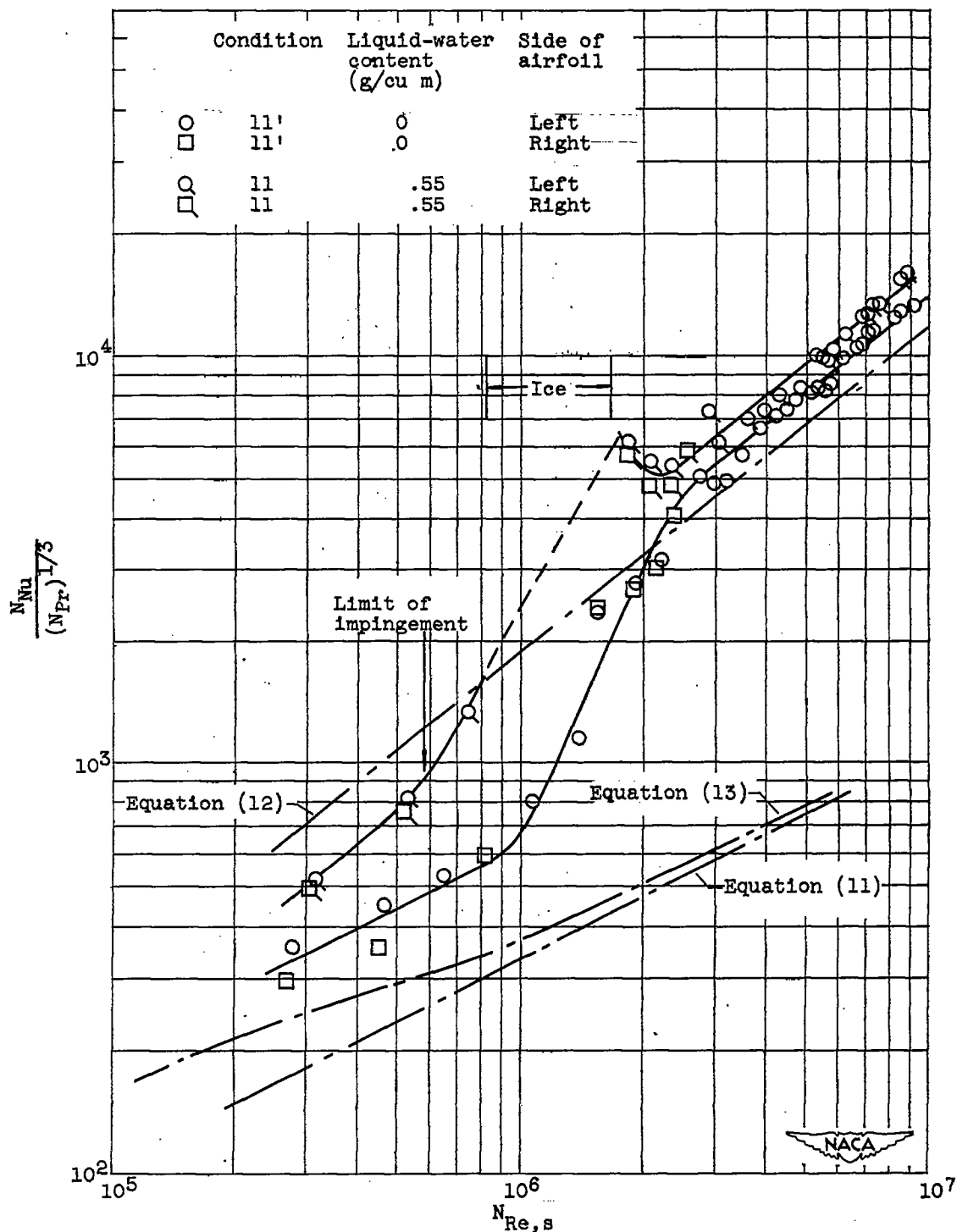
(a) Left side of airfoil.



(b) Right side of airfoil.

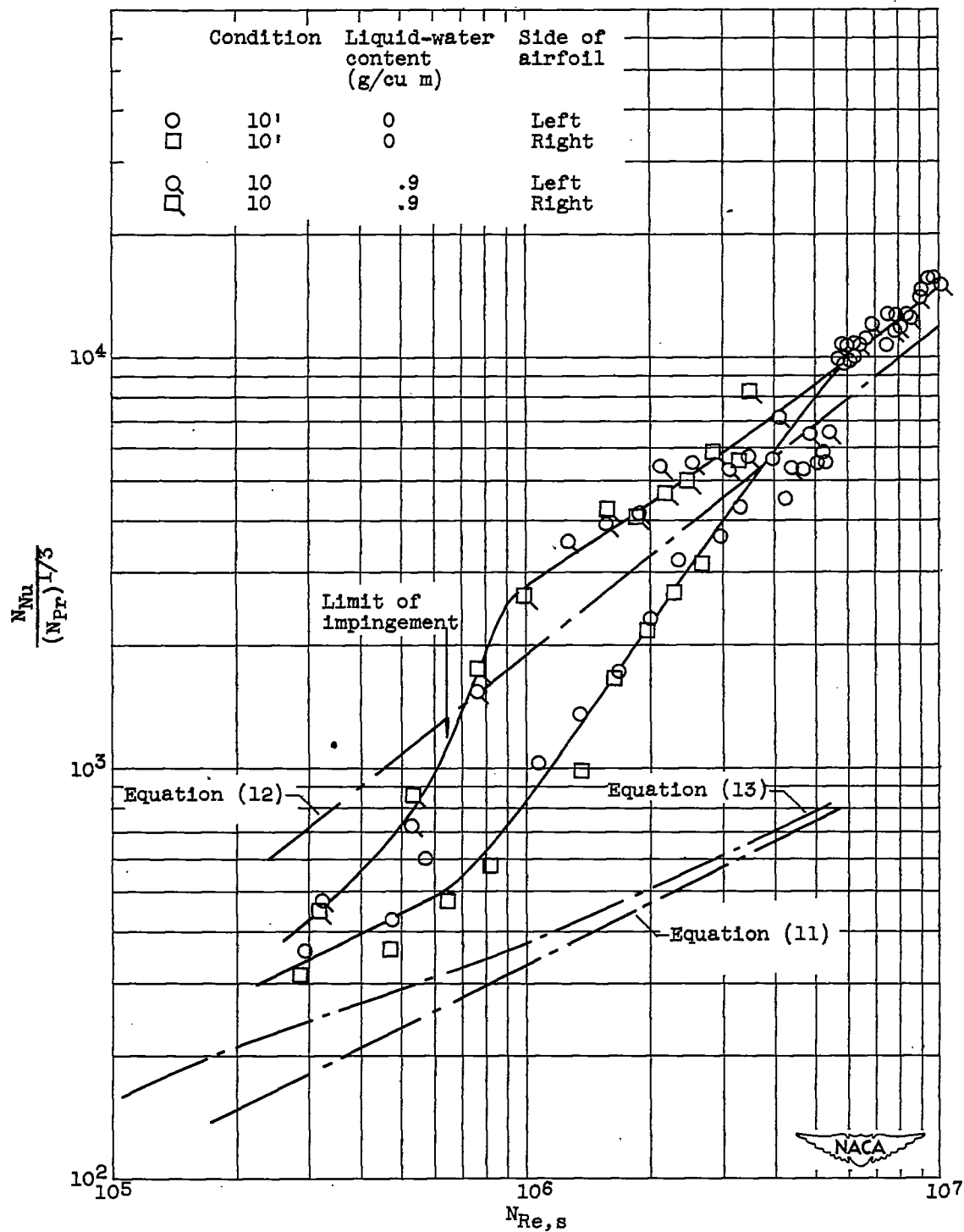

C-27480

Figure 16. - Ice formations on NACA 65,2-016 electrically heated airfoil model
in icing-tunnel. Condition 11.



(a) Conditions 11' and 11. Identical heating distributions resulting in nonuniform surface temperatures in icing but uniform surface temperatures in clear air.

Figure 17. - Correlation of heat-transfer data obtained in icing and in clear air in icing-research tunnel; spray system 48 feet upstream of model.



(b) Conditions 10' and 10. Identical heating distributions resulting in uniform surface temperatures in icing but nonuniform surface temperatures in clear air.

Figure 17. - Concluded. Correlation of heat-transfer data obtained in icing and in clear air in icing-research tunnel; spray system 48 feet upstream of model.

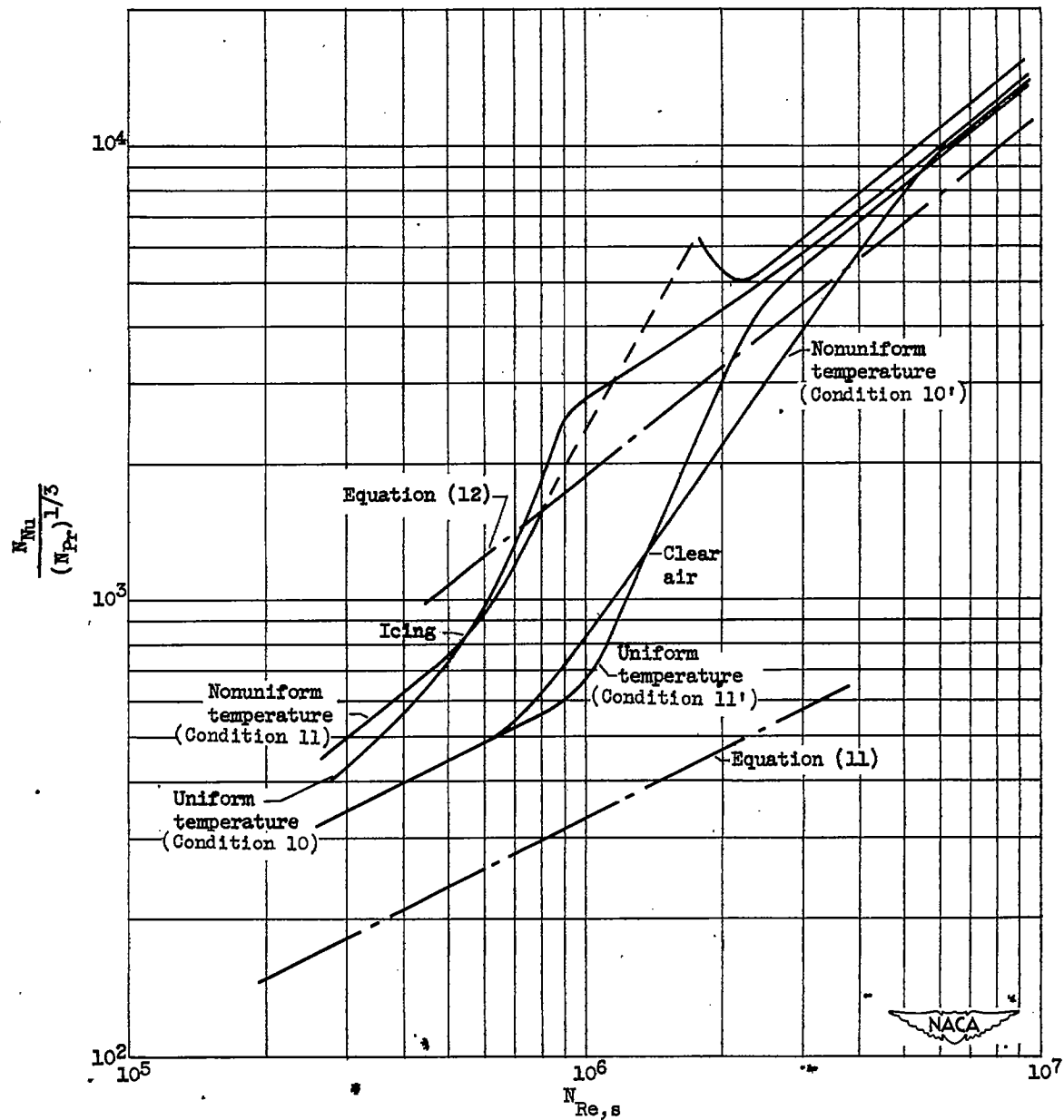


Figure 18. - Comparison of heat-transfer characteristics in icing-research tunnel. Tunnel heating distributions resulting in uniform surface temperatures in icing and in clear air with corresponding nonuniform surface temperatures in clear air and in icing. Conditions 10, 10', 11, and 11'.

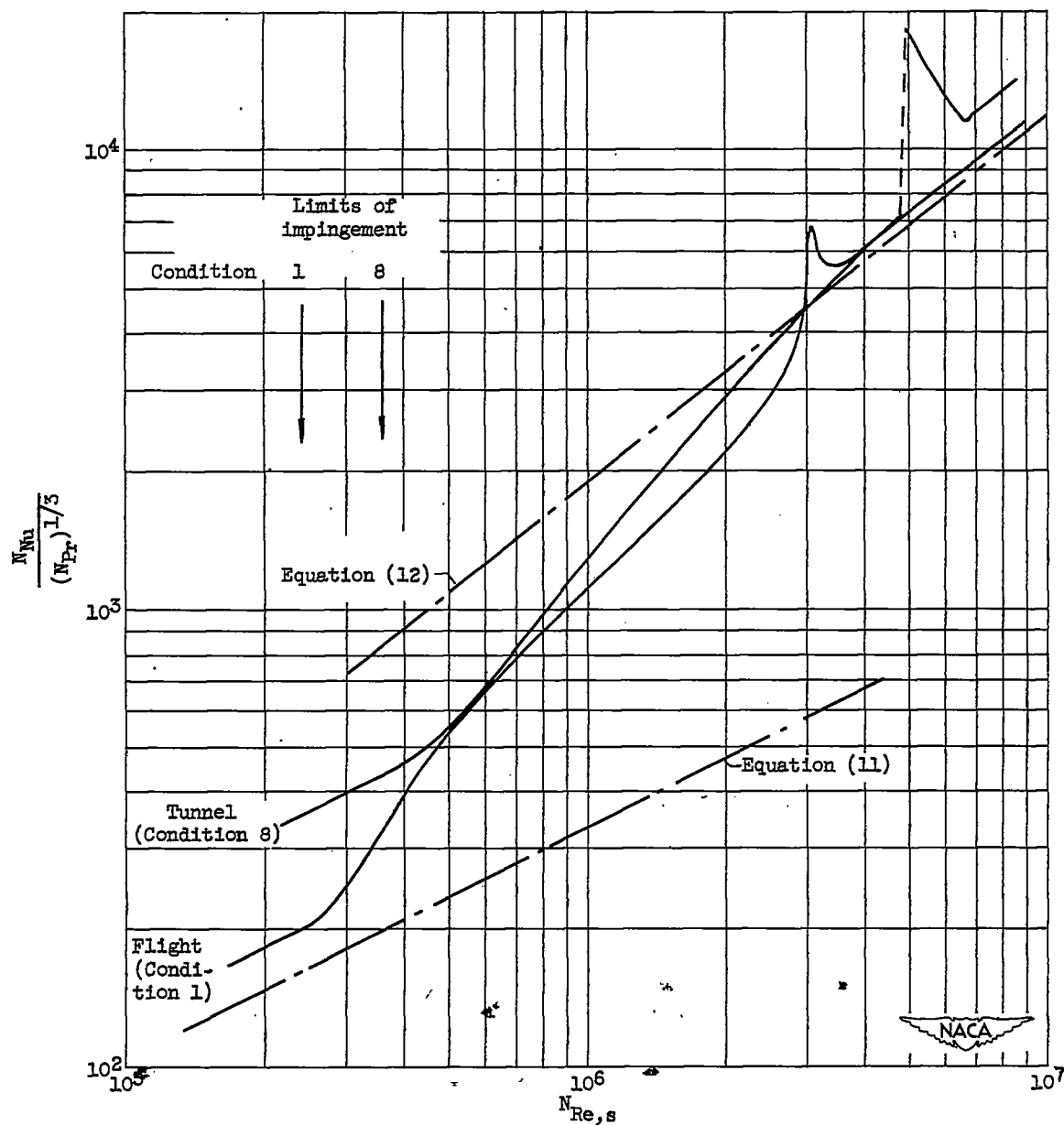


Figure 19. - Comparison of heat-transfer characteristics obtained in flight and in icing-research tunnel. Nonuniform surface temperatures, similar chordwise heating distribution, true airspeed, and free-stream temperature; NACA 65,2-016 electrically heated airfoil model; conditions 1 and 8.